

Original citation:

Gupta, A., Keddie, D.J., Kannappan, V., Gibson, H., Khalil, I.R., Kowalczyk, M., Martin, C., Shuai, X. and Radecka, I. (2019) Production and Characterisation of Bacterial Cellulose Hydrogels Loaded with Curcumin Encapsulated in Cyclodextrins as Wound Dressings. *European Polymer Journal*, 118, pp. 437 - 450, DOI: 10.1016/j.eurpolymj.2019.06.018

Permanent WRaP URL:

<https://eprints.worc.ac.uk/8344/>

Copyright and reuse:

The Worcester Research and Publications (WRaP) makes this work available open access under the following conditions. Copyright © and all moral rights to the version of the paper presented here belong to the individual author(s) and/or other copyright owners. To the extent reasonable and practicable the material made available in WRaP has been checked for eligibility before being made available.

Copies of full items can be used for personal research or study, educational, or not-for-profit purposes without prior permission or charge, provided that the authors, title and full bibliographic details are credited, a hyperlink and/or URL is given for the original metadata page and the content is not changed in any way.

Publisher's statement:

This is an Accepted Manuscript of an article published by Elsevier in *Pharmacological Research*, available online:

<https://www.sciencedirect.com/science/article/pii/S0014305719307803>. © 2019 Elsevier. Licensed under the Creative Commons Attribution-NonCommercial-NoDerivatives 4.0 International.

<http://creativecommons.org/licenses/by-nc-nd/4.0/>

A note on versions:

The version presented here may differ from the published version or, version of record, if you wish to cite this item you are advised to consult the publisher's version. Please see the 'permanent WRaP URL' above for details on accessing the published version and note that access may require a subscription.

For more information, please contact wrapteam@worc.ac.uk

1 **Production and characterisation of bacterial cellulose hydrogels loaded with curcumin**
2 **encapsulated in cyclodextrins as wound dressings**

3 A. Gupta^{a,c*}, D. J. Keddie^b, V. Kannappan^c, H. Gibson^{b,c}, I. R. Khalil^b, M. Kowalczyk^{b,c,e}, C.
4 Martin^d, X. Shuai^f, I. Radecka^{b,c*}

5 ^aSchool of Pharmacy, Faculty of Science and Engineering, University of Wolverhampton, Wulfruna Street,
6 Wolverhampton, WV1 1LY, UK.

7 ^bWolverhampton School of Sciences, Faculty of Science and Engineering, University of Wolverhampton,
8 Wulfruna Street, Wolverhampton, WV1 1LY, UK.

9 ^cResearch Institute in Healthcare Science, Faculty of Science and Engineering, University of Wolverhampton,
10 Wulfruna Street, Wolverhampton, WV1 1LY, UK.

11 ^dDepartment of Biological Sciences, Institute of Science and the Environment, University of Worcester, WR2
12 6AJ, UK.

13 ^eCentre of Polymer and Carbon Materials, Polish Academy of Sciences, M. Curie-Sklodowskiej 34, 41-819
14 Zabrze, Poland.

15 ^fPCFM Lab of Ministry of Education, School of Materials Science and Engineering, Sun Yat-sen University,
16 Guangzhou 510275, China

17 *Corresponding authors: a.gupta@wlv.ac.uk , I.Radecka@wlv.ac.uk

18 **Keywords:** Biosynthetic hydrogel, Curcumin, Cyclodextrin, Antimicrobial, Antioxidant,
19 Wound management

20 **Highlights**

- 21 • Curcumin:cyclodextrin-loaded cellulose based biosynthetic hydrogels were produced.
22 • These novel hydrogels exhibited haemocompatibility and cellular biocompatibility.
23 • CUR:HP β CD-loaded-bacterial cellulose showed antibacterial and antioxidant
24 properties.
25 • Acute and chronic wounds could benefit from their application.

26 **Abstract**

27 Natural bioactive materials with wound healing properties such as curcumin are attracting
28 interest due to the emergence of resistant bacterial strains. The hydrophobicity of curcumin
29 has been counteracted by using solubility enhancing cyclodextrins. Hydrogels facilitate
30 wound healing due to unique properties and 3D network structures which allows
31 encapsulation of healing agents. In this study, biosynthetic cellulose produced by
32 *Gluconacetobacter xylinus* (ATCC 23770) was loaded with water soluble
33 curcumin:hydroxypropyl- β -cyclodextrin supramolecular inclusion complex produced by a
34 solvent evaporation method to synthesise hydrogel dressings. The ratios of solvents to
35 solubilise curcumin and hydroxypropyl- β -cyclodextrin were tested for the production of the
36 inclusion complex with optimum encapsulation efficacy. The results confirmed that
37 hydroxypropyl- β -cyclodextrin enhanced the aqueous solubility of curcumin and allowed
38 loading into bacterial cellulose hydrogels. These hydrogels were characterised for wound
39 management applications and exhibited haemocompatibility, cytocompatibility, anti-
40 staphylococcal and antioxidant abilities and therefore support the potential use of the
41 curcumin:hydroxypropyl- β -cyclodextrin-loaded-bacterial cellulose as hydrogel dressings.

42 1. Introduction

43 Wound healing is a complex physiological process involving sequential yet overlaying
44 phases [1,2]. Correct clinical management of wounds is vital to minimise complications
45 during the healing process. The mandatory wound management requirements for all
46 wounds, no matter whether they are acute or chronic, involve control of infection, cleaning
47 the wound site and making it free from foreign material and necrotic tissue and the
48 selection of appropriate wound dressings [3]. Passive dressings *e.g.* gauze and tulle,
49 undoubtedly are inexpensive and provide a dry protective barrier, but cannot effectively
50 interact and respond to changing wound conditions [4]. An ideal dressing not only covers
51 and protects the affected area, but also optimises the wound environment to facilitate
52 healing [3,]. George Winter in 1960s established that the optimum moisture at the wound
53 site increases reepithelialisation and promotes healing [5]. This research revolutionised the
54 field of wound management, and the focus of wound dressings changed from conventional
55 dry passive products, to responsive moisture-promoting materials [4,5]. Following these
56 research findings, a wide range of dressings based on the moist healing concept were
57 developed with a range of different material compositions.

58 Hydrogels are one of the most promising candidates amongst the category of advanced
59 moist wound dressings. Hydrogels are composed of over 90% water [6] which is
60 responsible for their soft and malleable texture. In addition to acting as a barrier, hydrogels
61 facilitate healing by donating moisture in the case of dry necrotic wounds and absorbing
62 excessive exudate in the case of exudative wounds. This feature makes them capable of
63 creating the moist micro-climate between the wound bed and the dressing at the wound
64 site. Moreover, hydrogels reduce pain as a result of the cooling effect, allows exchange of
65 gases and can be loaded with antimicrobials and other healing agents [6,7].

66 Several cross-linked natural polymers like alginate, carboxymethyl cellulose, collagen,
67 chitosan and hyaluronic acid are in use as base materials for hydrogel dressings [1,8].
68 Bacterial cellulose (BC), a biosynthetic cellulose based polymeric hydrogel synthesised by
69 *Gluconacetobacter xylinus* has attracted wide interest in biomedical applications [9]. Its
70 hydrophilicity, biocompatibility, non-pyrogenic, high wet strength and transparency are
71 some of the desirable properties that resulted in its use for fabrication of several
72 proprietary wound dressings (XCell[®], Bioprocess[®], Dermafill[™], Gengiflex[®] and Biofill[®])
73 [7,9] with the clinical rationale being to facilitate autolytic debridement. BC's cross-linked
74 fibre network structure creates pores which allow impregnation of several healing agents
75 [7].

76 Natural products like curcumin (CUR), the curcuminoid present in turmeric, are becoming
77 more popular for regenerative medicine and wound management. CUR has multifaceted

78 mechanisms of action on wound healing [10] and less likely than presently used antibiotics
79 to develop resistant strains [11]. CUR (diferuloylmethane) (Fig. S1a in the supporting
80 information) is a naturally derived low molecular weight polyphenolic compound well
81 known for its pharmacological benefits like, but not limited to, anti-inflammatory, anti-
82 infective and anti-oxidant activities [10,11]. However, its hydrophobicity [11,12] limits its
83 biological activity for topical delivery for wound management applications.

84 Microencapsulation of medicinal substances in a suitable carrier is a common practice in
85 pharmaceuticals for drug delivery. Encapsulation can be used to protect the active
86 compound from the external environment, controlling delivery or to enhance the aqueous
87 solubility of the hydrophobic bioactive materials [13]. Cyclodextrins (CDs) are naturally
88 occurring cyclic oligosaccharide obtained from starch by enzymatic cyclisation that are
89 recognized as pharmaceutical adjuvants [14,15]. There are three commonly used native
90 cyclodextrins: α -cyclodextrin, β - cyclodextrin and γ - cyclodextrin with six, seven and
91 eight D-glucopyranose units linked by α -1,4 glycosidic bonds respectively. These linkages
92 of glucopyranose units result in truncated cone structures (Fig. S1b in the supporting
93 information). The primary and secondary hydroxyl groups located at the edges are
94 responsible for hydrophilic exterior surface of CDs. The skeletal carbons (C_3 and C_5) and
95 endocyclic acetal oxygen of glucose residues are oriented inside which imparts a
96 hydrophobic character to the interior CD cavity [16]. The polarity of the CD cavity has
97 been reported to be similar to an aqueous ethanolic solution [15]. Apart from naturally
98 occurring CDs, several chemically modified derivatives have been synthesized to improve
99 the properties (aqueous solubility, toxicological profiles *etc.*) of native CDs [15,17].

100 There are several studies reported on the enhancement of aqueous solubility of lipophilic
101 compounds by their inclusion in the CD cavity [12,13,18,19]. This can be achieved by
102 several techniques like co-precipitation, hot melt extrusion, solvent evaporation, freeze
103 drying, spray drying, slurry mixing, dry mixing *etc.* [14]. This study was conducted with
104 the aim of producing novel biosynthetic hydrogel dressings with healing properties. The
105 set objective was approached by encapsulation of CUR within hydroxypropyl- β -
106 cyclodextrin (HP β CD) to enhance its aqueous solubility leading to consistent loading in
107 the biosynthetic BC hydrogel matrix. The potential healing properties and the physical
108 performance characteristics of the CUR:HP β CD-loaded-BC hydrogels were investigated.

109 Herein, we describe the production of CUR:HP β CD-loaded-BC hydrogels for wound
110 management applications. Moreover, we discuss the effect of varied volume ratio of
111 solvents to dissolve CUR and HP β CD on encapsulation efficacy during CUR:HP β CD
112 inclusion complex (IC) formation using a solvent evaporation method. Qualitative and
113 quantitative characterization performed on the CUR:HP β CD and CUR:HP β CD-loaded-BC
114 hydrogels to assess their potential wound management applications is also discussed. As

115 far as the authors are aware, there are no studies reported in the literature on the
116 production and characterization of CUR:HP β CD-loaded biosynthetic BC hydrogels for
117 wound management applications.

118 2. Materials and Methods

119 2.1. Microorganisms, media and materials

120 *Gluconoacetobacter xylinus* (ATCC 23770) and *Staphylococcus aureus* (NCIMB
121 6571) were obtained from the University of Wolverhampton culture collection. Both
122 microorganisms were maintained at -20 °C in a lyophilised form. Stock culture of *G.*
123 *xylinus* was resuscitated on sterile mannitol agar (composition: yeast extract (5 g/L),
124 peptone (3 g/L), mannitol (25 g/L), agar (15 g/L); all materials were purchased from
125 Lab M, Bury, UK) and incubated for 48 h at 30 °C. Stock cultures of *S. aureus* were
126 resuscitated on sterile tryptone soy agar (TSA) (Sigma-Aldrich, UK), prepared
127 according to the manufacturer's protocol and sterilised by autoclaving prior to use,
128 and incubated for 48 h at 37 °C. Overnight broth cultures were aseptically prepared in
129 suitable broth using the stock plates prior to experimental use. Bacteriological
130 peptone, yeast extract and dextrose for the Hestrin and Schramm (HS) culture media
131 were purchased from Lab M (UK). HS media was prepared following the standard
132 protocol [20]. Tryptone soya broth (TSB), disodium phosphate and citric acid were
133 purchased from Sigma-Aldrich (UK).

134 A549 lung adenocarcinoma, U251MG glioblastoma, MSTO mesothelioma and Panc 1
135 pancreatic ductal adenocarcinoma were purchased from ATCC (UK).

136 Hydroxypropyl- β -cyclodextrin (parenteral grade) was obtained from Roquette
137 (France) and curcumin was purchased from Alfa Aesar (UK). Acetone was purchased
138 from Fischer Scientific (UK). D₂O was purchased from Goss Scientific (UK). Ringer
139 solution (1/4 strength) tablets were purchased from Lab M (UK) and prepared by
140 dissolving one tablet in 500 mL of de-ionised water and sterilised prior to
141 experimental use. Thiazolyl Blue Tetrazolium Bromide (MTT), sodium bicarbonate
142 and 2,2-diphenyl-1-picrylhydrazyl (DPPH) were purchased from Sigma-Aldrich
143 (UK). Dimethyl sulfoxide (DMSO), spectrophotometric grade, was purchased from
144 Alfa Aesar (UK). Sodium hydroxide was purchased from Acros Organics (UK). NaCl
145 (5.8 g/L) and glycine (7.6 g/L) were used for preparing Sorensen's glycine buffer and
146 purchased from Sigma-Aldrich, UK. Trypsin was purchased from Lonza (Belgium).
147 Dulbecco's Modified Eagle's Medium (DMEM), Fetal Bovine Serum (FBS), L-
148 Glutamine and Antibiotic Antimycotic (10,000 units/mL penicillin, 10,000 μ g/mL
149 streptomycin and 25 μ g/mL amphotericin B) were purchased from Gibco (UK).

150 **2.2. Preparation and characterisation of CUR:HP β CD inclusion complex**

151 **2.2.1. Preparation of CUR:HP β CD inclusion complex**

152
153 Inclusion complex of CUR with HP β CD was synthesised by the solvent
154 evaporation (SE) method at the molar ratio of 1:1, following the protocol
155 report by Yallapu, Jaggi, & Chauhan, (2010) [18], with appropriate
156 modifications. In the current study, an attempt was made to prepare
157 CUR:HP β CD inclusion complex by varying the volume ratio of solvents and
158 evaluating the effect on encapsulation efficacy.

159 Briefly, CUR (0.79 g) was dissolved in acetone (5 mL) and HP β CD (3.0 g)
160 was dissolved in deionised water (45 mL). CUR solution was added dropwise
161 to the aqueous HP β CD solution under constant stirring in a Schott bottle
162 covered with aluminium foil. As the volume ratio of acetone to water was 10
163 %, this sample was designated as IC 10. Similarly, using the same amounts of
164 material (CUR 0.79 g and 3.0 g HP β CD) while varying the solvent volume
165 ration, IC 25 (CUR in 12.5 mL acetone and HP β CD in 37.5 mL water); IC 50
166 (CUR in 25 mL acetone: HP β CD in 25 mL water), IC 75 (CUR in 37.5 mL
167 acetone: HP β CD in 12.5 mL water) and IC 90 (CUR in 45 mL acetone:
168 HP β CD in 5 mL water) were prepared (Table. 1). Stirring was performed in a
169 fume hood at room temperature for up to 72 h by replacing the lids of Schott
170 bottles with perforated aluminium foil to allow acetone to slowly evaporate.
171 Samples were then centrifuged at 3000 rpm for 10 min and the supernatant
172 containing water soluble inclusion complex of CUR:HP β CD was collected.
173 The resultant inclusion complex was filtered through a 0.45 μ m filter
174 (MILLEX[®] HA, Merck Millipore) to remove any free CUR. The aqueous
175 solution of ICs were then frozen at -20 °C overnight and lyophilised to obtain
176 solid powders which were stored in dark for further experimental use.

177 **Table 1: Summary of the preparation of CUR:HP β CD inclusion complexes by varying**
178 **the volume ratio of solvent.**

Inclusion complex	Mass of CUR (g)	Mass of HPβCD (g)	Volume of acetone to dissolve CUR (mL)	Volume of water to dissolve HPβCD (mL)
IC 10	0.79	3.00	5.00	45.00
IC 25	0.79	3.00	12.50	37.50
IC 50	0.79	3.00	25.00	25.00
IC 75	0.79	3.00	37.50	12.50
IC 90	0.79	3.00	45.00	5.00

179 **2.2.2. Characterisation of CUR:HPβCD inclusion complex**

180 The formation of the inclusion complex was confirmed by testing its
181 physicochemical properties. In addition to the studies presented in this section,
182 further characterisations like morphological study by SEM, chemical
183 characterisation by FTIR were undertaken which are presented in section
184 2.3.3.

185 **2.2.2.1. Solubility study**

186 CUR, HPβCD and CUR:HPβCD (10 mg each) were weighed and
187 added to deionised water (10 mL) in separate universal tubes. These
188 were stirred for 1 h at room temperature (22 °C) followed by
189 filtration using 0.45 μm filter. An aliquot was taken for UV-Visible
190 spectrophotometric scan between 350-650 nm.

191 **2.2.2.2. Determination of curcumin content and Encapsulation**
192 **Efficiency (EE)**

193 CUR content in the inclusion complex was quantified by using UV-
194 Visible spectroscopy at a wavelength of 430 nm. The wavelength of
195 430 nm is the λ_{max} of CUR without any interference absorbance
196 from HPβCD [21]. CUR:HPβCD (1 mg) was dissolved in dimethyl
197 sulfoxide (DMSO) (5 mL) and gently shaken in an orbital shaker at
198 150 rpm at 37 °C for 1 h to extract CUR. The solution was filtered
199 through 0.45 μm filter and CUR content was determined by UV-
200 Visible spectroscopy at 430 nm. A standard calibration plot of CUR
201 in DMSO was produced as a reference. The Encapsulation
202 Efficiency (%) was determined using the formula:

$$\% EE = \frac{\text{mass of encapsulated curcumin}}{\text{mass of curcumin initially used}} \times 100$$

203

204

205 **2.2.2.3. X-ray diffractometric analysis (XRD)**

206 The X-ray diffraction patterns of CUR, HPβCD and CUR:HPβCD
207 were obtained by an X-ray diffractometer (Empyrean, PANalytical,
208 Neitherslands) with Cu radiation source. The X-ray diffractometer
209 was set at a voltage of 40 kV and current of 40 mA.

210
211
212
213
214
215
216
217
218
219
220
221
222
223
224
225
226
227
228
229
230
231
232
233

2.2.2.4. Nuclear magnetic resonance (NMR)

The NMR experiments including ^1H , proton-decoupled ^{13}C , homonuclear correlation spectroscopy (COSY), heteronuclear single quantum correlation (HSQC), heteronuclear multiple bond correlation (HMBC), and rotating-frame nuclear Overhauser spectroscopy (ROESY) were performed on a 400 MHz JEOL NMR spectrometer JNM-ECZ400R/M1. The sample consisted of 10-20 mg of the inclusion complex dissolved in deuterium oxide. All spectra were internally referenced to residual solvent [22]. ^1H spectra were acquired with a 45° pulse and inter-pulse delay of 5 seconds across 16 transients with acquisition time of 2.18628 seconds and pulse width of 6.48 μs ; ^{13}C NMR spectra were recorded with a 30° pulse and inter pulse delay of 5 seconds across 4097 transients with acquisition time of 1.03809 seconds, and pulse width of 10.338 μs ; HSQC spectra were recorded using a matrix consisting of 256×819 points across eight scans with a relaxation delay of 3 seconds; HMBC spectra were recorded using a matrix consisting of 512×1638 points across eight scans with a relaxation delay of 3 seconds; COSY spectra were recorded by using a matrix of 1024×1024 points across 1 scan with a relaxation delay of 3 seconds; ROESY spectra were recorded in a phase sensitive mode with 1024 points in the x direction and 256 points in the y direction and acquired with 4 scans and relaxation delay of 1.5 seconds. Mixing time value was 0.25 seconds.

234
235
236
237
238
239
240
241

2.2.2.5. Thermal gravimetric analysis (TGA)

The evaluation of the thermal properties of CUR, HP β CD and CUR:HP β CD and physical mixture of CUR and HP β CD was undertaken using a Mettler Toledo Thermogravimetric Analyzer, TGA/DSC 1 STAR[®] System. Samples were subjected to TGA from 25 $^\circ\text{C}$ to 800 $^\circ\text{C}$ at 10 $^\circ\text{C}/\text{min}$ under constant flow of nitrogen (60 mL per minute). Differential thermogravimetry (DTG) curve was also studied as a first derivative of TGA curve.

242
243
244
245

2.2.2.6. Differential scanning calorimetry (DSC)

DSC scans of CUR, HP β CD, CUR:HP β CD and physical mixture of CUR and HP β CD were performed using DSC Q2000 (TA instruments, New Castle, DE). The scans were collected using

246 aluminum pans (TA instruments) with a nitrogen flow rate of 50
247 mL/min and temperature ramp rate of 20 °C/min.

248

249 **2.3. Preparation and characterisation of CUR:HP β CD-loaded-BC hydrogels**

250 **2.3.1. Preparation of BC hydrogel pellicles**

251 Bacterial cellulose (BC) hydrogel pellicles were prepared and purified by the
252 protocol reported previously [7]. Briefly, *G. xylinus* was selected for
253 biosynthesis of BC and grown in the Hestrin and Schramm (HS) culture
254 medium under static condition by incubation at 30°C for 14 days.
255 Biosynthesised pellicles were harvested after this period and purified by firstly
256 boiling in 1% (w/v) aqueous sodium hydroxide and subsequently in deionised
257 water until the BC became clear and transparent.

258 **2.3.2. Loading CUR:HP β CD inclusion complex in BC hydrogel pellicles**

259 It is important to note that due to the highest encapsulation efficacy, IC 75 was
260 selected for loading and further characterisation. Purified BC pellicles were
261 padded dry using filter paper and loaded with IC 75 by immersing in 2 %
262 (w/v) aqueous solution of CUR:HP β CD overnight under constant agitation at
263 37 °C. Sterile conditions were maintained throughout the loading process.

264 **2.3.3. Characterisation studies**

265 CUR:HP β CD-loaded-BC hydrogels produced after loading the inclusion
266 complex in padded dry BC were characterised to evaluate their properties for
267 the potential wound dressing applications.

268 **2.3.3.1. Scanning electron microscopy (SEM)**

269 Solid samples of BC, CUR, HP β CD, CUR:HP β CD and lyophilised
270 samples of CUR:HP β CD-loaded-BC were coated with gold using
271 SC500 fine coater (Emscope, Kent, UK). The shape and
272 morphology of these samples was studied using Zeiss Evo 50 EP,
273 SEM (Carl Zeiss AG, Oberkochen, Germany).

274

2.3.3.2. Fourier transform infrared (FTIR) spectroscopy

275

276

277

278

279

FTIR of CUR, HP β CD, CUR:HP β CD and CUR:HP β CD-loaded-BC was recorded using a FTIR spectrophotometer (Bruker, Alpha, Platinum-ATR). The scanning range used was 400-4000 cm⁻¹ with 16 scans settings for each sample run. A background scan was run prior to the scan of samples to obtain spectra.

280

2.3.3.3. Moisture content (M_c)

281

282

283

284

285

The wet mass (W_w) of BC (neat BC hydrogels) and BC hydrogel pellicles loaded with aqueous solution of CUR:HP β CD (2 % w/v) was determined before lyophilisation and the dry mass (W_d) was recorded after lyophilisation. M_c (%) was calculated using a formula:

$$\% M_c = \frac{(W_w - W_d)}{W_w} \times 100$$

286

2.3.3.4. Optical Transmission and Transparency test

287

288

289

290

291

292

293

294

295

296

The quantitative optical transmission (%) of hydrogels was determined using LI-250A Light meter (LI-COR[®] Biosciences). BC pellicles were padded dry and rehydrated either with deionised water (neat BC) or 2 % (w/v) aqueous solution of CUR:HP β CD (test hydrogels) and optical transmission (% T) of light was read. Readings were taken for petri dish with deionised water (control), neat BC pellicles in petri dish and test BC pellicles. Four readings from a different sections of each neat and test BC pellicles were recorded and averages used to examine the % T by comparison to the control (100 % T).

297

298

299

300

301

Moreover, the neat and 2 % CUR:HP β CD-loaded-BC hydrogels were transferred on the laminated paper with text in different colours. The clarity of letters beneath each hydrogel was examined to determine if it would permit observation and assessment simulating to wound monitoring context.

302
303
304
305
306
307
308
309
310
311
312
313
314
315
316
317
318

319
320
321
322
323
324
325
326
327
328
329
330

331
332

333
334
335
336
337

2.3.3.5. Water vapour transmission rate (WVTR)

The WVTR of neat BC and CUR:HPβCD-loaded-BC hydrogel dressings was measured using the cup test method according to the American Society for Testing and Materials (ASTM) standard [23,24]. In the current study, to achieve controlled conditions with minimum variations in set parameters during the entire length of the experiment, hypoxia incubator (Optronix, Oxford, UK) was used instead of saturated salt chamber as reported previously [25]. An incubator temperature of 35±0.1 °C and 60±1 % relative humidity [RH] was maintained using compressed air during the entire period of the experiment. There was no attempt to artificially adjust air flow in the chamber as the influence of local air velocity was not examined in this study. A digital balance (ON BALANCE™, Myco MZ-100-BK) was placed inside the chamber for weighing the assemblies. The selected temperature (35 °C) corresponds to the temperature of the wound site as reported by Lamke *et al.*, 1977 [26].

Purified BC pellicles were padded dry and rehydrated either with deionised water (neat BC) or 2 % (w/v) CUR:HPβCD aqueous solution (test hydrogels) under agitated conditions at 150 rpm and 37 °C overnight in an orbital shaker. Thickness of the rehydrated BC pellicles was measured using a Vernier calliper (Whitworth Digital calliper). Four readings for each pellicle were taken and average thickness calculated. Neat BC and/or CUR:HPβCD-loaded-BC hydrogels (2.44 cm exposed diameter) were secured onto glass vessels containing 7.5 mL distilled water. The assemblies were kept in the chamber in upright position. WVTR was determined (in triplicates) by weighing the complete beaker assembly inside the chamber at set time intervals and calculated as [27]:

$$WVTR = \frac{\text{slope} \times 24}{\text{test area in m}^2} \text{ g/m}^2/\text{day}$$

2.4. *In vitro* tests of CUR:HPβCD-loaded-BC hydrogels

2.4.1. Haemocompatibility

In the current study, with the intended wound management applications, the haemocompatibility of CUR:HPβCD-loaded-BC hydrogels was evaluated *in vitro*, by assessing haemolytic potential of hydrogels. The test was performed as previously reported for testing haemocompatibility of BC with some modifications [25]. Briefly, defibrinated horse whole blood (purchased from

338 TCS Biosciences Ltd) was washed with sterile 0.9 % saline (pH 5.5) twice and
339 centrifuged at 3000 rpm for 10 min before re-suspending in saline solution. 2
340 % (w/v) CUR:HPβCD was prepared in saline and loaded in padded dry BC
341 pellicles. Using the biopsy punch, CUR:HPβCD-loaded-BC discs (≈8.0 mm)
342 were cut and incubated with 1.9 mL saline-suspended horse blood cells in test
343 Eppendorfs under sterile conditions. Positive (+ve) controls were distilled
344 water suspended blood cells and negative (-ve) controls were blood cells
345 suspended in saline. Eppendorfs were incubated at 4 °C for 2 h with gentle
346 inversion after every 15 min. Post-incubation, BC discs were removed under
347 sterile condition followed by each sample being centrifuged at 3000 rpm for
348 10 min and supernatant decanted. Absorbance was recorded at 540 nm and
349 percentage (%) haemolysis was determined as follows:

$$\% \text{ Haemolysis} = \frac{(\text{Abs of sample}) - (\text{Abs of -ve control})}{(\text{Abs of +ve control}) - (\text{Abs of -ve control})} \times 100$$

350 **2.4.2. Cytocompatibility (*in vitro* cell viability)**

351 Cytocompatible nature of BC has been previously reported [25]. To study the
352 effect of the CUR:HPβCD-loaded-BC on cell viability, the previously reported
353 study was extended on 4 human cancer cell lines from different tissues,
354 namely, A549 (human lung adenocarcinoma), MSTO (human mesothelioma),
355 PANC1 (human pancreatic ductal adenocarcinoma) and U251MG (human
356 glioblastoma).

357 All cell lines were cultured in DMEM medium containing 4.5 g/L glucose,
358 supplemented with fetal bovine serum (10 %), Antibiotic Antimycotic (1 %),
359 L-Glutamine (2 mM) and incubated at 37 °C in a humidity incubator with 5 %
360 CO₂. The cytocompatibility of free CUR:HPβCD and CUR:HPβCD-loaded-
361 BC was investigated. Four different concentrations of CUR:HPβCD (1 %, 1.25
362 %, 1.5 %, 2 % w/v) were prepared in Dulbecco's Modified Eagle's Medium
363 (DMEM). BC pellicles were padded dried and either rehydrated with DMEM
364 (control) or the respective concentrations of CUR:HPβCD in DMEM (test) in
365 an orbital shaker at 37 °C at 150 rpm for overnight. Discs (≈8.0 mm diameter)
366 were cut from the control and test pellicles using a corer for the experimental
367 purposes. The whole procedure was conducted aseptically.

368 Briefly, 25,000 cells per well were seeded in 24 well plates for 24 h at 37 °C in
369 5% CO₂ incubator. The cells were then exposed to either free CUR:HPβCD or
370 CUR:HPβCD-loaded-BC discs for 24 h. After incubation, the morphology of
371 cells, confluence of the cell monolayer and cell viability was observed
372 microscopically using an inverted light microscope (Nikon, Japan). The effect

373 of free CUR:HP β CD and CUR:HP β CD-loaded-BC discs on cell viability was
374 evaluated by standard MTT cytotoxicity assay by adding 5 mg/ml MTT
375 solution (Sigma, UK) in all the wells and incubated for 2 h, followed by
376 solubilising the formazan crystals with DMSO and Sorensen's glycine buffer
377 (pH 10.5). All experiments were done in triplicates and cell viability was
378 calculated using the mean absorbance measured at 540 nm and the results were
379 statistically analysed by two-way ANOVA with a Tukey's multi comparisons
380 test using GraphPad Prism.

381 **2.4.3. Curcumin release study**

382 Small (\approx 8.0 mm diameter) sized discs of purified BC were cut using a biopsy
383 punch and padded dry on filter paper. These discs were loaded with 2 % (w/v)
384 aqueous solution of CUR:HP β CD by incubating overnight at 37 °C in glass
385 Bijoux bottles, under agitated conditions at 150 rpm.

386 These discs were transferred to individual Bijoux tube containing 1 mL 0.9 %
387 saline (pH 5.5) and incubated under static conditions at 35 °C. At set intervals,
388 discs were moved to a new set of bijoux tubes with fresh 1 mL saline and
389 incubated under same conditions. This was repeated over 48 h and CUR
390 release was spectroscopically assessed at 430 nm for each time interval.

391
392 The standard calibration curve of CUR in 0.9 % saline (pH 5.5) was produced
393 as a reference. Briefly, the stock solution (1000 μ g/mL) of CUR was prepared
394 by taking CUR (10 mg) and dissolving in ethanol:saline (70:30 % v/v) and
395 making up to 10 mL. A standard solution (30 μ g/mL) was prepared by taking
396 150 μ L of stock solution and making up to 5.0 mL using saline. Using this
397 standard solution, other standards were prepared in saline and the standards
398 were read at 430 nm using saline as blank.

399 400 **2.4.4. Antimicrobial activity by disc diffusion assay:**

401 The antimicrobial activity of BC loaded with 2 % (w/v) aqueous CUR:HP β CD
402 was investigated against *S. aureus*, using the disc diffusion assay; purified BC
403 and BC loaded with HP β CD were used as controls. Discs of BC, BC-HP β CD
404 and BC-CUR:HP β CD (\approx 8.0 mm diameter) were aseptically cut and placed on
405 TSA plates spread with overnight culture of *S. aureus* and following
406 incubation at 37 °C for 24 h, the zone of inhibition (ZOI) was measured.
407 Results are presented for ZOI (mm) at 24 h and analysed by one-way ANOVA
408 with a Tukey's multi comparisons test using GraphPad Prism.

409 **2.4.5. Anti-oxidant activity by DPPH assay**

410 2,2-diphenyl-1-picrylhydrazyl (DPPH) radical scavenging assay was
411 performed according the protocol reported by [28] with appropriate
412 modification. Briefly, test solutions of varying concentrations of CUR:HP β CD
413 in methanol were prepared and methanol was used in preparing a blank. The
414 assay mixture with 1 mL DPPH (80 μ g/mL) methanolic solution and 1 mL
415 solutions of various concentrations of the material (including a blank) after
416 mixing were incubated in dark for 30 min at room temperature. Absorbance
417 was measured spectrophotometrically at 517 nm. The free radical scavenging
418 capacity was calculated as percent antioxidant effect (% E) using the following
419 equation. Different sample concentrations were used to produce a curve for
420 calculating IC₅₀ values, the amount of sample required to obtain 50 % of the
421 free radical inhibition [29].
422

$$\%E = \frac{Abs_{control} - Abs_{sample}}{Abs_{control}} \times 100$$

423

424

425 3. Results and discussion

426 3.1. Preparation of CUR:HP β CD-loaded-BC hydrogels

427 *G. xylinus* produced BC hydrogel pellicles in 2 weeks under static conditions. These
428 pellicles were harvested and purified to get rid of entrapped bacterial cells and excess
429 media. The hydrogel pellicles after purification became clear and transparent (Fig. 1a)
430 which is in accordance with our previous study [7]. The BC pellicles after purification
431 were ready for loading with CUR:HP β CD.

432 CUR:HP β CD (yellow powder) was produced from the CUR (dark yellow powder)
433 and HP β CD (white powder) by solvent extraction method which is in accordance with
434 the literature [18]. The novel approach taken in this study to produce IC 10, IC 25, IC
435 50, IC 75 and IC 90, supramolecular inclusion complexes revealed that varied solvent
436 volume ratios have an influence on CUR content encapsulated in HP β CD. The EE
437 (%) results of IC 10, IC 25, IC 50, IC 75 and IC 90 revealed 3.64 ± 0.16 %, 3.84 ± 0.37
438 %, 7.37 ± 1.24 %, 18.26 ± 1.02 % and 16.34 ± 0.75 % (n=3) encapsulation efficacy
439 respectively. These results suggested that IC 75 produced by CUR dissolved in 37.5
440 mL acetone and HP β CD dissolved in 12.5 mL water for the inclusion complex
441 production gave highest % EE hence it was selected as a standard procedure for the
442 preparation of inclusion complex for further experimental investigations. It is
443 important to note that all the characterisations for CUR:HP β CD were done using IC
444 75. CUR content determined in IC 75 samples was in the range of 3.28 ± 0.38 % (n=4).

445 IC 75 was loaded in padded dry BC to produce hydrogels for wound management
446 applications. Visual inspection of purified BC hydrogel pellicles loaded with 2 %
447 (w/v) CUR:HP β CD revealed highly consistent loading (Fig. 1b). After loading of the
448 inclusion complex, the colour of BC hydrogels changed from clear to orange yellow
449 (Fig. 1a-b).

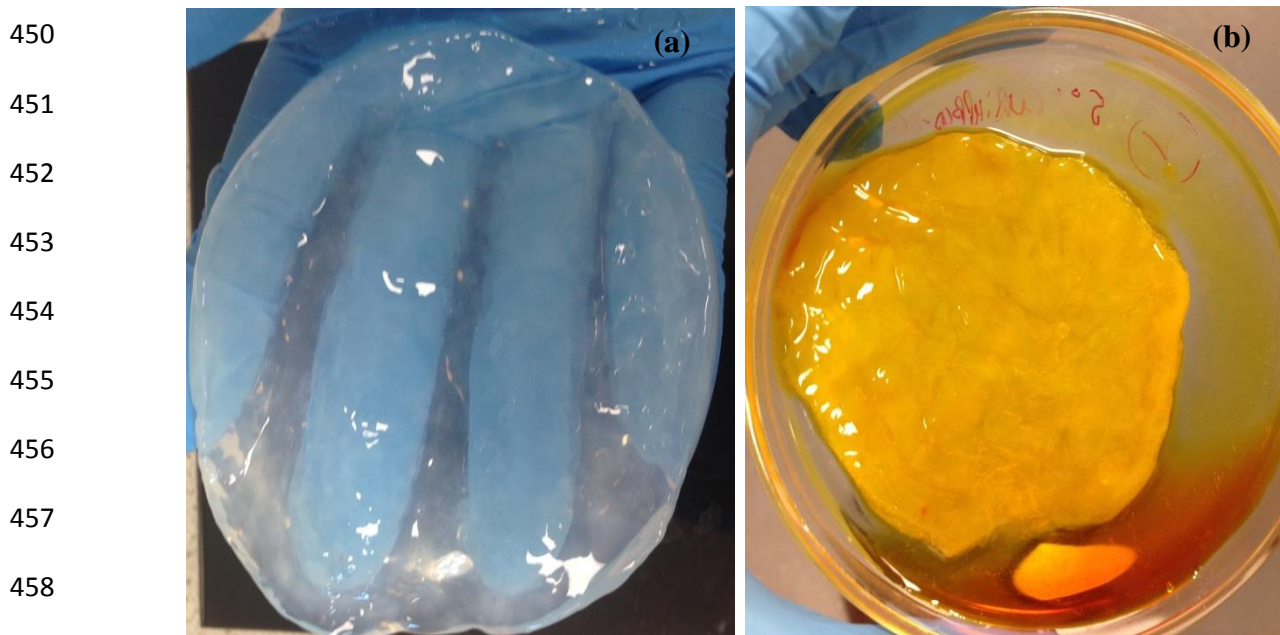


Figure 1: Visual appearance of (a) BC hydrogel pellicle after purification
(b) CUR:HP β CD-loaded-BC hydrogel pellicle.

459 **3.2. Characterisation studies of CUR:HP β CD inclusion complex and CUR:HP β CD-**
460 **loaded-BC hydrogels**

461 **3.2.1. Solubility in water: CUR versus CUR:HP β CD inclusion complex**

462 CUR exhibits the maximum absorbance at ≈ 430 nm [30]. In the current study,
463 the inclusion of CUR in HP β CD enhanced its aqueous solubility which was
464 evident in the spectral scan (Fig. 2). The UV-Visible spectrum of aqueous
465 filtrate of CUR didn't exhibit significant absorption in the specified spectral
466 range suggesting low aqueous solubility of CUR at the aforesaid conditions.
467 Moreover, the aqueous solution of HP β CD didn't show significant absorbance
468 in the selected range. In case of the CUR:HP β CD, there was strong
469 absorbance recorded around 430 nm due to enhanced aqueous solubility of
470 CUR. These results correspond with previous studies that CUR has poor
471 aqueous solubility which could be enhanced by its inclusion in CD cavity
472 [19,31,32].

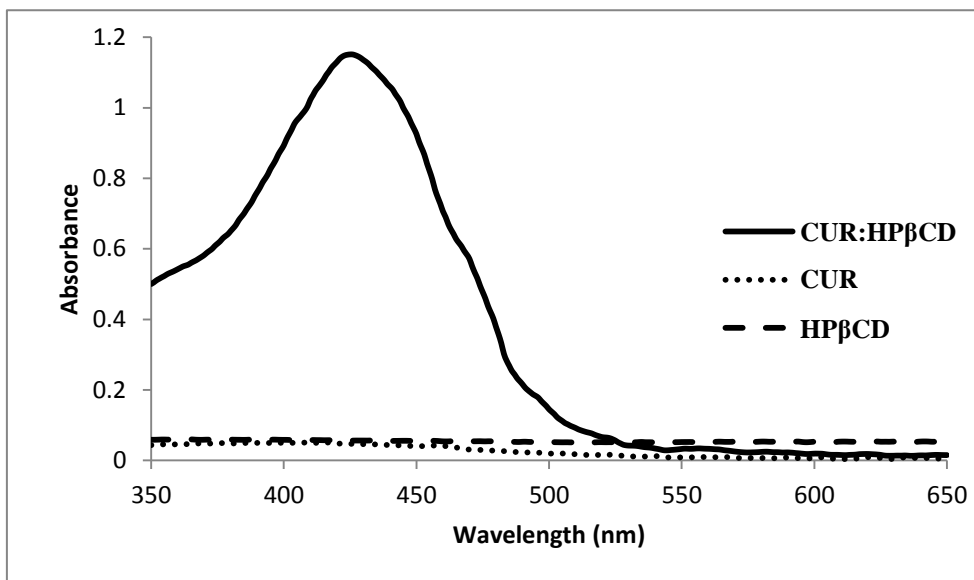


Figure 2: UV-Visible absorption spectra of CUR, HP β CD and CUR:HP β CD dissolved in water after 1 h stirring at room temperature followed by filtration through 0.45 μ m filter.

473
474

475

3.2.2. X-ray Diffractometric analysis (XRD)

476

477

478

479

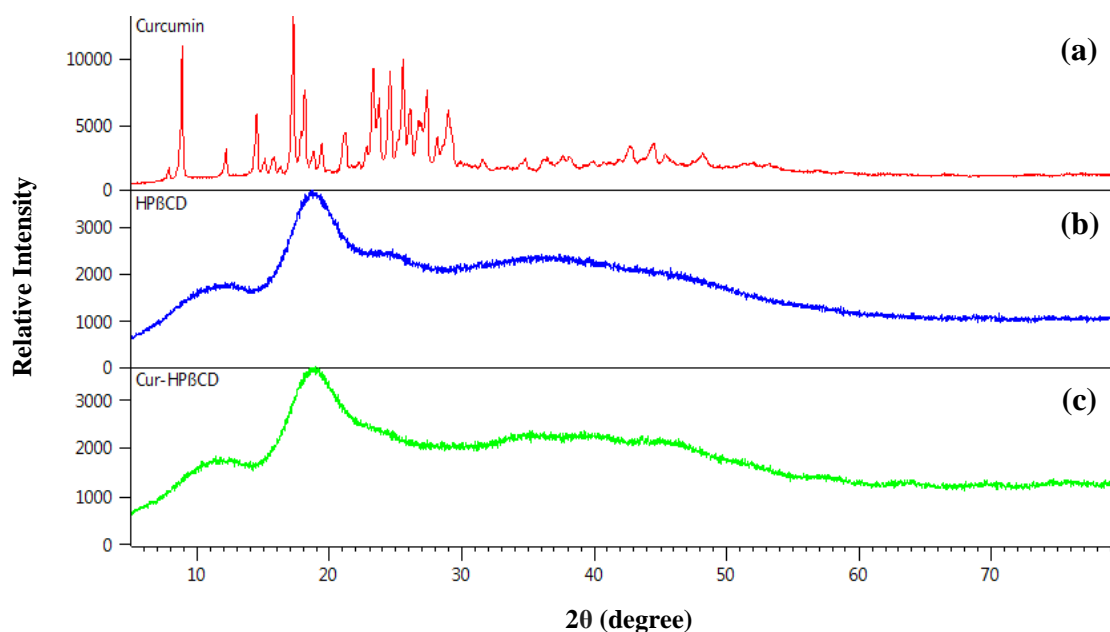
480

481

482

483

The XRD spectra of CUR, HP β CD and lyophilised CUR:HP β CD are shown in Fig. 3. Results revealed that CUR exists in a crystalline form which is indicated by the characteristic peaks (Fig. 3a) whereas HP β CD is amorphous (Fig. 3b) in nature. After complexation with HP β CD, there was no noticeable evidence of crystallinity of CUR in the inclusion complex (Fig. 3c). This suggests that CUR may have formed an inclusion complex with HP β CD leading to the loss of peaks. These results are in accordance with literature findings [19,33,34].



484

Figure 3: XRD results of (a) CUR (b) HP β CD (c) CUR:HP β CD.

485

3.2.3. Nuclear Magnetic Resonance spectroscopy (NMR)

486

487

488

489

490

491

NMR spectroscopy was used to investigate the success of the formation of the inclusion complex between hydroxypropyl- β -cyclodextrin and curcumin (sample IC 75). The ^1H and ^{13}C NMR data of the CUR:HP β CD was assigned using a combination of previously reported proton NMR data [35] and 2D NMR techniques (COSY, HSQC and HMBC) (see Fig. S2-S5 in the supporting information).

492

493

494

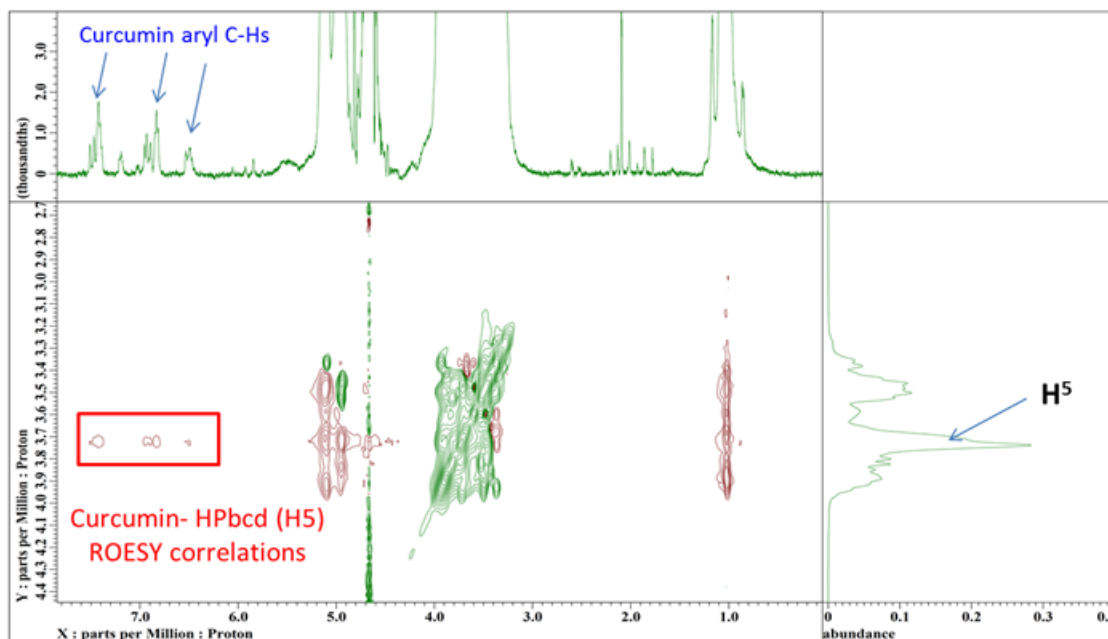
495

496

Evidence for the formation of the CUR:HP β CD inclusion complex can be chiefly observed through both ^1H and ROESY NMR. Comparison between the ^1H NMR spectra of HP β CD and CUR:HP β CD shows a distinctive shift in the proton resonances of the internally facing protons, H 3 and H 5 of HP β CD upon inclusion of CUR indicating a change in the local magnetic environment; the

497 resonances of the externally facing protons remained unchanged (Fig. S6 and
498 S7; see Scheme S1a-c for structural assignments in the supporting
499 information).

500 Further conclusive evidence for the formation of CUR:HP β CD was
501 subsequently obtained by ROESY NMR analysis; a ROESY correlation
502 between H⁵ of HP β CD and CUR aryl protons spectrum clearly indicates a
503 through space interaction indicative of an inclusion complex (Fig. 4).



504 **Figure 4:** Expansion of the ROESY spectrum of the CUR:HP β CD inclusion
505 complex in D₂O indicating correlation cross peaks between HP β CD and CUR.

506 3.2.4. Thermal Analysis (TGA and DSC)

507 The thermal analytical techniques like TGA and DSC are widely used in pre-
508 formulation studies. The thermokinetic data could be used to understand the
509 thermal decomposition reaction and helps determine the storage conditions.
510 Moreover, the comparison of TG curves of pure compounds, their physical
511 mixture and the CUR:HP β CD inclusion complex could provide evidence of
512 interactions between compounds and the formation of inclusion complex [36].

513 Thermal behaviour of CUR, HP β CD, CUR:HP β CD was investigated and
514 compared to CUR and HP β CD physical mixture, to understand the solid-state
515 characterisation and thermal stability of the inclusion complex during
516 production and storage. Thermogravimetric data revealed that thermal
517 degradation of CUR starts at around 220 °C, which is \approx 40 °C above its
518 melting point. It loses around 54 % mass between 300-420 °C. HP β CD mass

519 loss of nearly 6 % at around 91 °C attributed to the loss of water and major
520 mass loss (>70 %) peaks at 344 °C due to the decomposition of the molecule
521 (Fig. 5a-b). These weight losses were visible in both, the physical mixture and
522 CUR:HPβCD inclusion complex. On further examination, it was noticed that
523 the inclusion complex displayed higher thermal stability as shown in Fig. 5a-b
524 but as our study aims at the application of the product at the physiological
525 temperature so the decomposition at high temperatures (>300 °C) was not
526 significant. It should be noted that due to the inclusion of CUR in HPβCD
527 cavity, the thermal behaviour of CUR was different from free CUR which is in
528 accordance with literature [36].

529 The thermokinetic data did not show decomposition at normal working
530 temperatures suggesting that the production and storage of the inclusion
531 complex at room temperature does not affect its thermal stability. BC is
532 thermally stable at the standard autoclaving temperatures [25]. The data from
533 the current study suggests that the inclusion complex is also thermally stable at
534 such temperatures. Since BC and the inclusion complex are both thermally
535 stable at the standard autoclaving temperatures, the hydrogel dressings may be
536 sterilised by autoclaving prior to the application on the wound site.

537 DSC analysis was performed to further corroborate the results obtained from
538 TGA. DSC results of CUR revealed an enthalpy change with a sharp
539 endotherm in the region of 179 °C indicative of its melting point (Fig. 5c). In
540 the case of HPβCD, there was observed two endotherms around 259 °C and
541 291 °C followed by its decomposition (Fig. 5c). In the case of physical
542 mixture, the characteristic endotherms of CUR appeared at 179 °C suggesting
543 free CUR in the physical mixture. Moreover, endotherm peaks attributed to
544 HPβCD were also visible. However, shift in peak positions was observed (Fig.
545 5c) which could be due to the interactive effect of HPβCD with CUR on
546 mixing, which is in accordance with literature findings [19]. The thermogram
547 of CUR:HPβCD revealed that the melting endotherm peak for CUR in the
548 inclusion complex disappeared, suggesting that CUR was protected up to 244
549 °C. Moreover, the shift in endotherm peaks attributed to HPβCD in
550 CUR:HPβCD inclusion complex was observed. This may be due to molecular
551 interactions of inclusion of CUR in the HPβCD cavity (Fig. 5c) thus indicating
552 the formation of the inclusion complex.

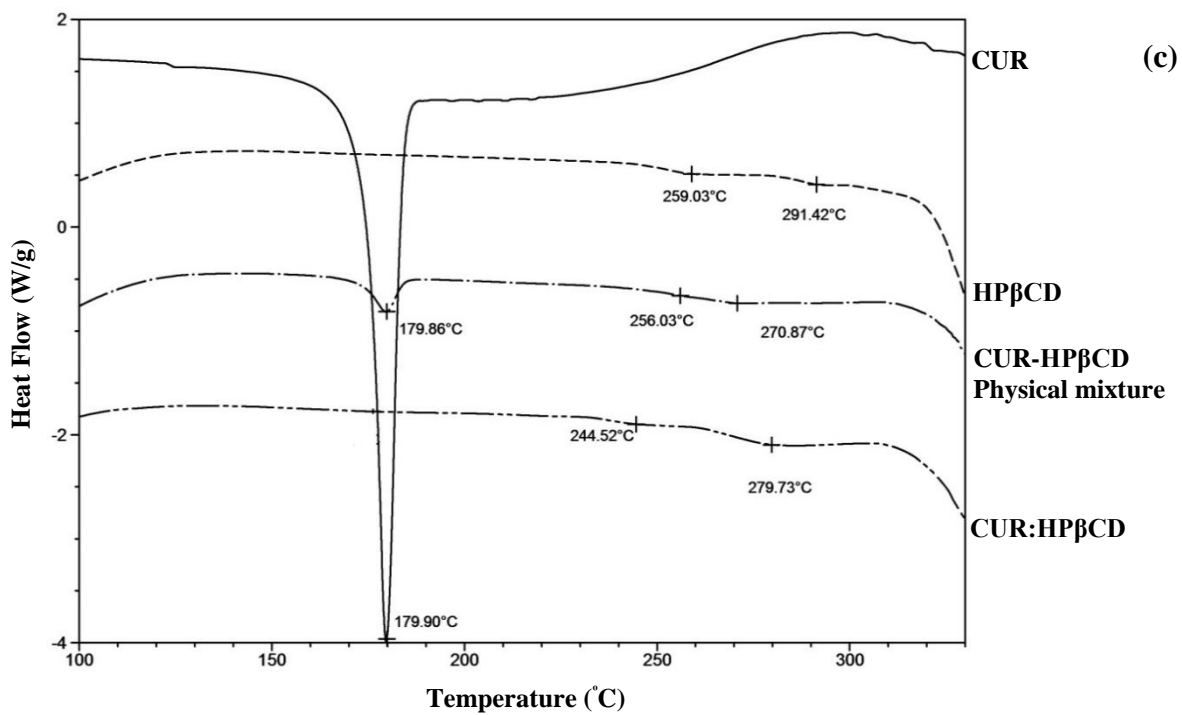
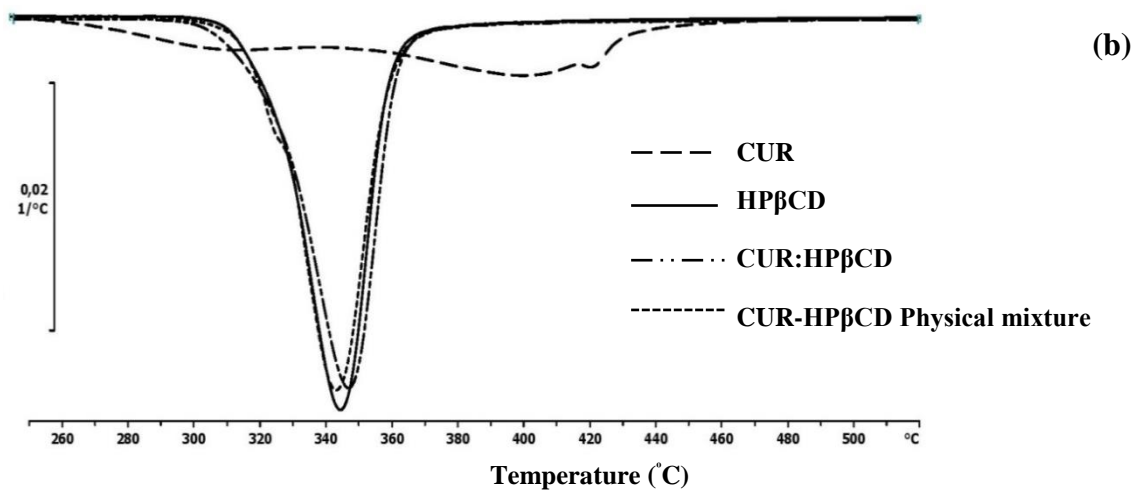
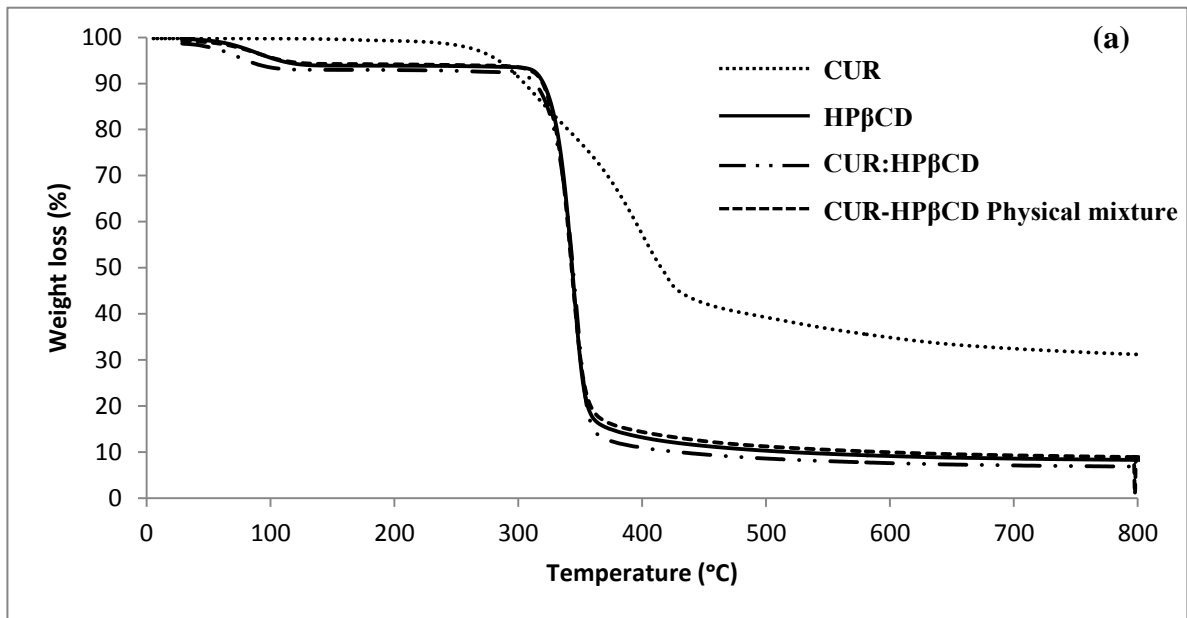


Figure 5: (a) TGA curves (b) DTG curves (c) DSC spectra of CUR, HPβCD, CUR, HPβCD Physical mixture and CUR:HPβCD.

554 **3.2.5. Scanning electron microscopy (SEM)**

555

556 BC appears as a dense interwoven fibre network [7]. It emerged that the fine
557 ribbons (30-105 nm thickness) (Fig. 6a) of cellulose entangle with each other
558 forming the network structure interspersed with voids. Morphological studies
559 of lyophilised purified BC revealed two types of pores in the BC network
560 structure; nano pores with pore size as low as 27 nm (Fig. 6b) and some large
561 superficial pores with diameter value of up to 10 μm (Fig. 6c). It may be noted
562 that these pores may further expand on hydration with water. SEM results
563 revealed that the shape of CUR and HP β CD changed from round to irregular
564 shape to plate like structures in CUR:HP β CD (Fig. 6d-f). When padded dry
565 BC was rehydrated by immersion in aqueous solution of CUR:HP β CD, the
566 voids allowed penetration of the inclusion complex which then got physically
567 entrapped in the BC fibre network (Fig. 6g). This resulted in the production of
568 CUR:HP β CD-loaded-BC hydrogels.

569

571

3.2.6. Fourier transform infrared (FTIR)

572

573

574

575

576

577

578

579

580

581

582

583

584

585

586

A detailed investigation on the vibrational spectra of CUR, HP β CD and BC has been reported in literature [7,19,32]. FTIR spectral results of CUR, HP β CD, CUR:HP β CD, purified BC and CUR:HP β CD-loaded-BC are illustrated in Fig. 7. The characteristic sharp peak at 3504 cm⁻¹ and a broad peak at band regions of 3308 cm⁻¹ suggested the presence of OH; 1619 cm⁻¹ was assigned to C=C and C=O vibrations; 1591 cm⁻¹ to the stretching vibrations of benzene ring and 1497 cm⁻¹ to the C=C (Fig. 7a). For HP β CD the characteristic broad peak at 3340 cm⁻¹ was assigned to stretching vibrations of OH group; 2927 cm⁻¹ to C-H stretching and other prominent peaks presented at 1156 cm⁻¹ and 1084 cm⁻¹ (C-H), 1024 cm⁻¹ (C-O-C glucose units) (Fig. 7b). In CUR:HP β CD, due to the encapsulation of CUR in HP β CD cavity, the peaks of CUR appeared to be masked or shifted. The prominent peaks at 3504 cm⁻¹ and 1619 cm⁻¹ appeared to be masked by HP β CD molecular vibrations in the inclusion complex (Fig. 7c) which could be due to the inclusion of CUR in HP β CD cavity [19,31,32].

587

588

589

590

591

BC has characteristic peaks at 3342 cm⁻¹, 2899 cm⁻¹, 1640 cm⁻¹, 1370 cm⁻¹, 1159 cm⁻¹, 1057 cm⁻¹ (Fig. 7d). These peaks appeared in CUR-HP β CD-loaded-BC spectra (Fig. 7e). Furthermore, the characteristic peaks of the inclusion complex were also observed in the spectra (Fig. 7e), thereby confirming the loading of the inclusion complex in the BC network.

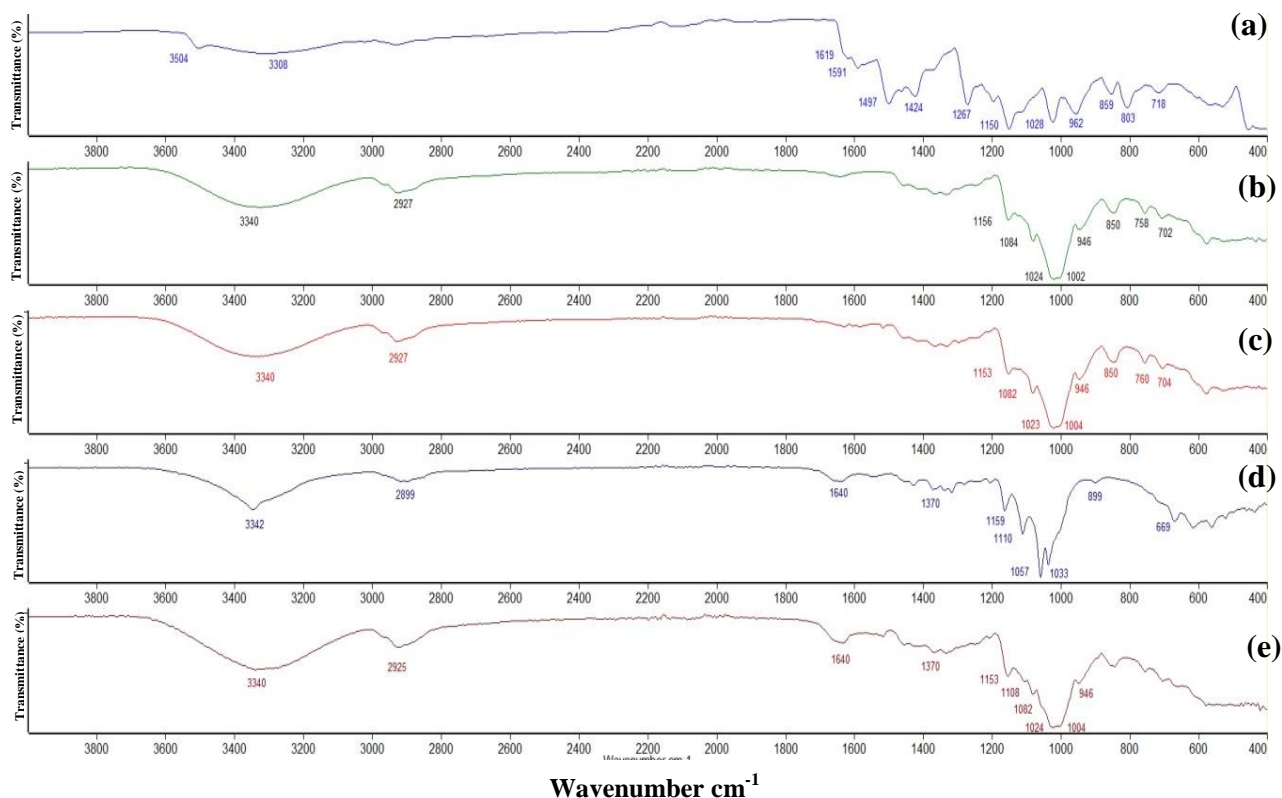


Figure 7: FTIR spectra from 400-4000cm⁻¹ for (a) CUR (b) HP β CD (c) CUR:HP β CD (d) bacterial cellulose (e) CUR:HP β CD-loaded-BC.

592 3.2.7. Moisture content (M_c)

593 BC hydrogels have high water content and the results of the moisture content
594 determination study revealed neat BC hydrogels imbibed $>99.5\%$ ($n=4$) water
595 which is accordance with previously published data [25]. Moreover, the results
596 revealed that BC loaded with 2% (w/v) CUR:HP β CD imbibed $97.63\pm 0.057\%$
597 ($n=4$) water. These results suggested that CUR:HP β CD inclusion complex that
598 gets physically trapped in BC fibres (as suggested in Fig. 6g) contributes to
599 this difference between neat BC and CUR:HP β CD-loaded-BC.

600 Wound dressings with high moisture content offers several benefits including,
601 but not limited to, high malleability, easy and pain free removal of the
602 dressing, cooling and soothing effect resulting in a sensation of pain reduction
603 with a capability of developing a moist microclimate that has been proven to
604 enhance epithelialisation [1,3,5,37,38]. The high moisture content in
605 CUR:HP β CD-loaded-BC hydrogels produced in the current study would
606 deliver these beneficial attributes and contributes towards facilitating wound
607 healing along with patient comfort and compliance.

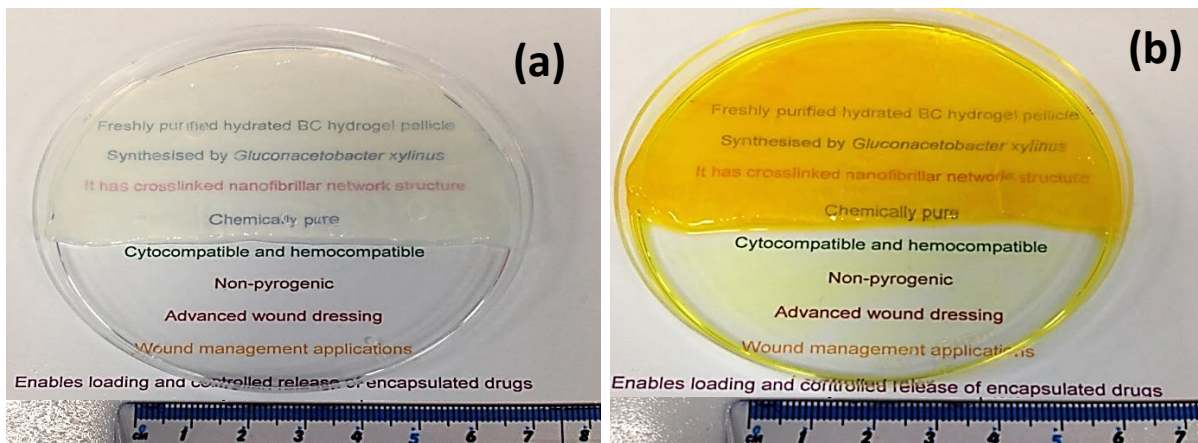
608 3.2.8. Optical Transmission and Transparency test

609 The appearance of the wound site is vital to assess patients' response to the
610 treatment. A basic technique to carry out this assessment is by visual
611 observation of the wound site by the removal of the dressing, however removal
612 of the dressing from the wound site could cause trauma [3]. Non-invasive
613 monitoring of the healing process without the need to remove the wound
614 dressing has the potential to ensure effective management [39]. This would
615 allow regular clinical assessment of the wound healing process, improve
616 patient comfort and potentially lower the cost of treatment with less frequent
617 dressing change.

618 Transparency is a property that measures the ability of the material to allow
619 the light pass through without scattering [40]. In the current study an attempt
620 was made to produce the hydrogel dressings delivering this feature. Neat BC
621 hydrogels demonstrated the % Transmission of $85.72\pm 1.57\%$ ($n=3$).
622 Although, the light transmittance of CUR:HP β CD-loaded-BC hydrogel
623 dressings was reduced, this is sufficiently high ($66.13\pm 2.36\%$) ($n=3$).

624 On further evaluation, the clarity of letters through the hydrogels supported
625 high transparency through both the neat and CUR:HP β CD-loaded-BC
626 hydrogels (Fig. 8). These results support the capability of CUR:HP β CD-
627 loaded-BC hydrogel dressings for non-invasive clinical wound monitoring.

628 Several protocols have been reported in the literature to evaluate the
 629 transparency of hydrogels with wound dressing applications [37,41]. The
 630 authors are mindful that the method designed and employed in the current
 631 study for transparency testing may not exactly mirror the real wound site; for
 632 that to be considered, this study could be extended to *in vivo* animal models.
 633 Nevertheless, this method has several advantages due to its simplicity and low
 634 cost.



635 **Figure 8:** Visual appearance of text through (a) neat BC sheet (b) 2% CUR:HPβCD-loaded-BC.

636 3.2.9. Water Vapour Transmission Rate (WVTR)

637 Normal skin has the ability to control the water loss by evaporation from the
 638 body, to prevent dehydration, which gets compromised when the integrity of
 639 the skin is affected by injury. Lamke, Nilsson, & Reithner, 1977 [26] reported
 640 the evaporation water loss of $204 \pm 12 \text{ g/m}^2/24 \text{ h}$ from the normal skin which
 641 could go up to $5138.4 \pm 201.6 \text{ g/m}^2/24 \text{ h}$ in case of a granulating wound.

642 An ideal wound dressing material must have a property to control the
 643 evaporative water loss from the wound [24]. High WVTR may lead to
 644 dehydration and scab formation whereas very low WVTR may lead to the
 645 accumulation of exudate, maceration of periwound skin and increased risk of
 646 infections [38].

647 In the current study, WVTR was evaluated as the gradient of weight loss from
 648 the samples versus time. The thickness of rehydrated hydrogels (neat and test)
 649 was in the range of 1.5-2.5 mm. WVTR values for neat BC were in the range
 650 of $2526.32\text{-}3137.68 \text{ g/m}^2/24 \text{ h}$ (n=3) and for 2 % CUR:HPβCD-loaded-BC
 651 were $2258.53\text{-}2460.63 \text{ g/m}^2/24 \text{ h}$ (n=3). Previous reported studies suggest that
 652 a WVTR level of $2000\text{-}2500 \text{ g/m}^2/24 \text{ h}$ would be sufficient to maintain an
 653 optimum moist environment at the wound site [24,25,42]. Our results revealed
 654 that the WVTR range of CUR:HPβCD-loaded-BC hydrogels were close to the

655 recommended range hence would be suitable for wound healing applications.
656 Moreover, the results revealed that the loss of water from neat BC hydrogels
657 was more than from the test hydrogels (CUR:HP β CD-loaded-BC). We
658 postulated this is due to the CUR-HP β CD loaded in the BC network structure
659 reducing the void space in the hydrogels and controlling the transmission of
660 water in CUR:HP β CD-loaded-BC hydrogels compared to neat BC.

661 **3.3. *In vitro* characterisation of CUR:HP β CD-loaded-BC hydrogels**

662 **3.3.1. Biocompatibility studies (Haemocompatibility and Cytocompatibility)**

663 When materials come in contact with blood, they may cause haemolysis of the
664 blood cells thus assessment of haemolytic properties become vital for
665 materials with potential biomedical applications. According to the ASTM
666 F756 standards [43], haemolytic indices, the test samples can be: (a)
667 haemolytic materials with haemolysis >5 % (b) slightly haemolytic with
668 haemolysis between 2-5 % and (c) non-haemolytic materials having
669 haemolysis below 2 % [44]. The *in vitro* blood compatibility results revealed
670 that the test hydrogels are haemocompatible with % haemolysis <0.20 %
671 (n=9) which is well below the acceptable limit for haemolysis. These results
672 confirmed that CUR:HP β CD-loaded-BC hydrogels are non-haemolytic
673 material and suitable for wound management applications.

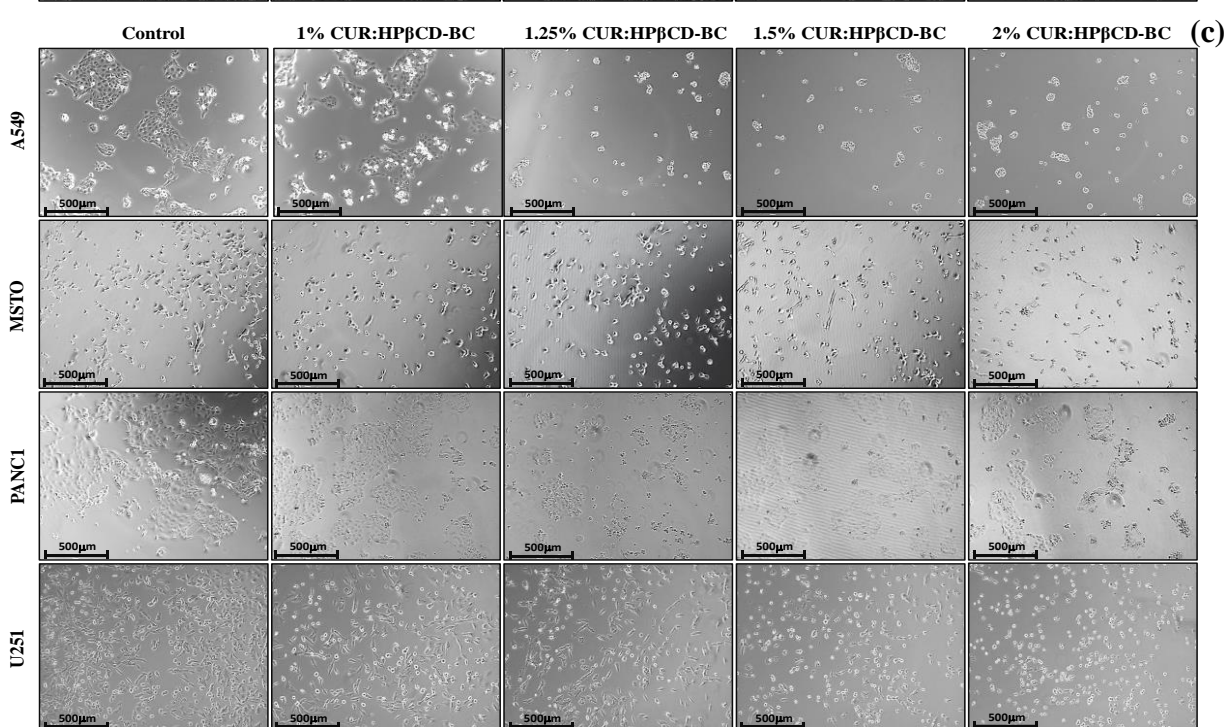
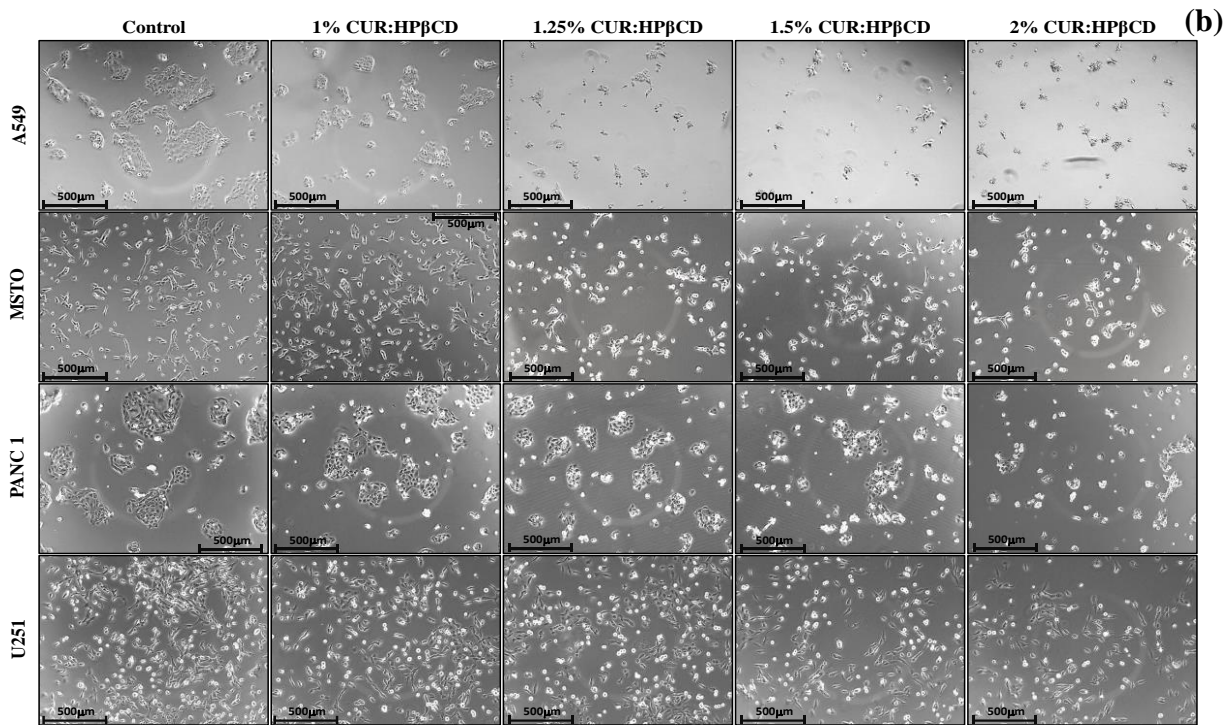
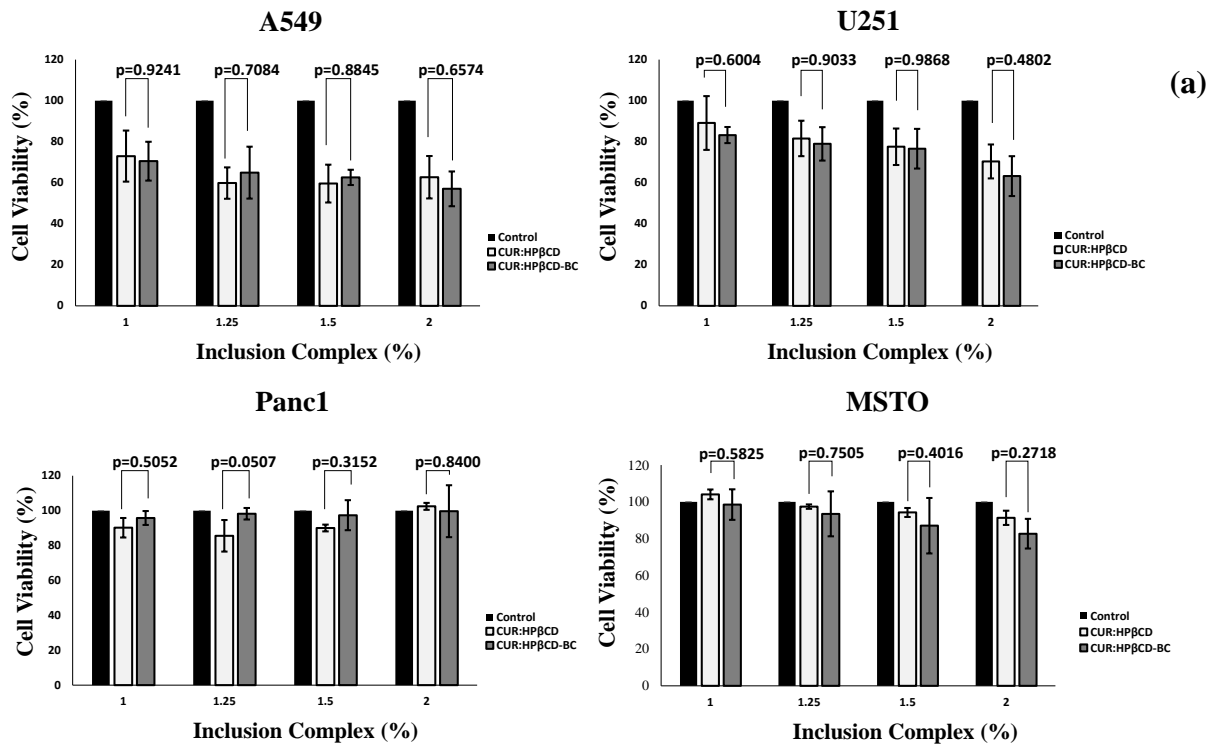
674 BC has been reported to be cytocompatible for biomedical applications
675 [25,37]. Cytocompatibility is one of the many properties of BC leading to its use
676 in fabricating proprietary wound dressings. High bacterial burden at the wound
677 site has deleterious effect on the wound healing hence the use of antimicrobial
678 becomes imperative. Since bacteriostatic and/or bactericidal agents may have
679 harmful effect on the host cells, therefore a benefit:risk ratio has to be
680 evaluated for the selection of antimicrobial wound dressings [45]. The use of
681 proprietary silver dressings in chronic wound management to control the
682 microbial bioburden is a good example where the benefit outweighs the risk of
683 cytotoxic effect of silver [45,46]. In the current study, the MTT
684 cytocompatibility study aims to find out how the CUR released from the
685 hydrogels affects the survival of mammalian cells. The cytotoxicity as
686 determined by MTT assay demonstrated that the CUR:HP β CD-loaded-BC
687 hydrogels has varied compatible with the tested cell lines (Fig. 9a). Despite
688 the varied response, all cell lines demonstrated cell viability when exposed to
689 CUR:HP β CD or CUR:HP β CD-loaded-BC hydrogels (Fig. 9a-c). Four
690 different cell lines were used in this study and most of them tolerated up to 2%
691 CUR:HP β CD over 24hrs and showed very good survival rates. Despite being
692 very sensitive, the A549 cell line also showed around 60 % survival at the
693 highest tested dose (2 %). Although this will be a significant decrease in cell

694 survival in comparison to control, this dose has not even reached the standard
695 IC50/50% cell death to define this as a highly toxic effect. Moreover, in
696 patients, this will correspond to how much free CUR is being released from
697 the material and get in the systemic circulation. It is very unlikely that this
698 amount will cause the toxic effect to vital organs.

699
700 Furthermore, we compared the cytocompatibility of CUR:HP β CD-loaded-BC
701 hydrogels with that of free CUR:HP β CD (equivalent amount). The results
702 showed that there was no significant difference ($p>0.05$) between the free
703 CUR:HP β CD or the 2 % CUR:HP β CD-loaded-BC hydrogels. This indicated
704 that the BC matrix used to deliver CUR:HP β CD inclusion complex does not
705 affect the cell viability.

706 Our results are in accordance with other cytotoxicity studies reporting the
707 cytocompatible nature of CUR and its conjugates for biomedical applications
708 [47-49]. These findings further support the potential wound dressing
709 applications of CUR:HP β CD-loaded-BC hydrogels.

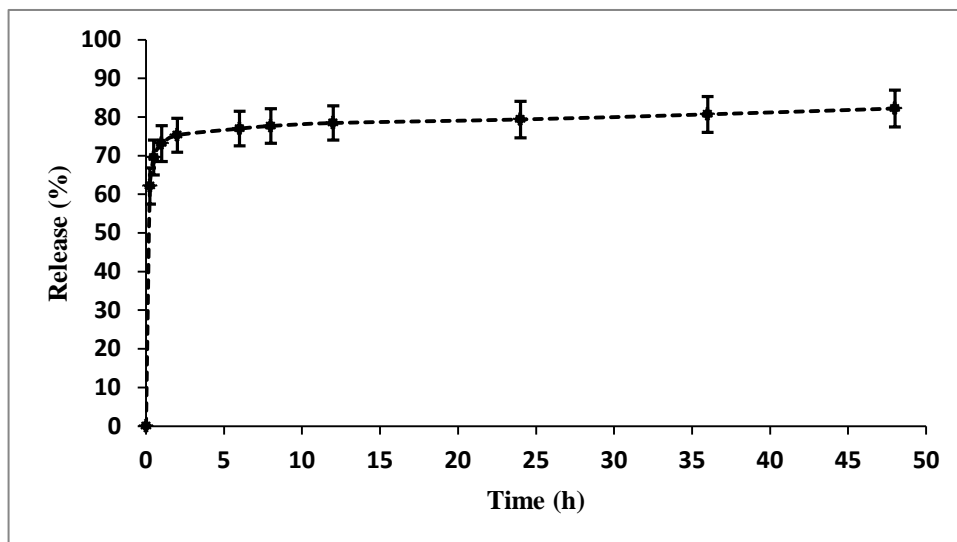
710



711 **Figure 9:** Cytocompatibility test results. Bar graphs showing viability of different cells after 24
712 h exposure to (a) free CUR:HP β CD and 2 % CUR:HP β CD-loaded-BC. Representative optical
713 photomicrographs of cells captured at 10x magnification after exposure for 24 h to (b) free
714 CUR:HP β CD (c) 2 % CUR:HP β CD-loaded-BC.

715 3.3.2. CUR release and Antimicrobial study

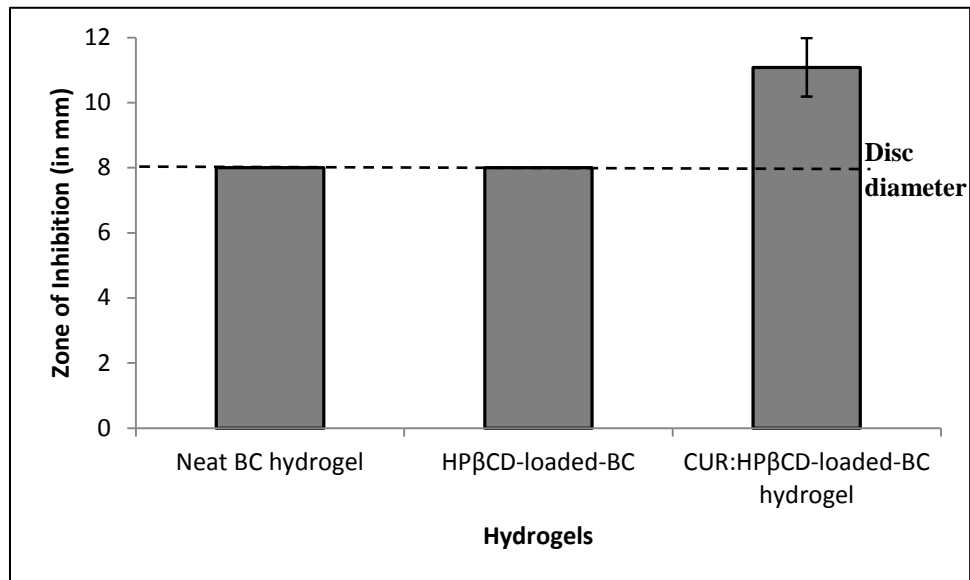
716 CUR release from CUR:HP β CD-loaded-BC hydrogels, as determined by UV-
717 Vis spectroscopy, is presented in Fig. 10. Results indicate that 76.99 ± 4.46 %
718 release (n=6) was achieved after 6 h from CUR:HP β CD-loaded-BC hydrogels.
719 The release was slow after this duration and reached 79.36 ± 4.71 % at 24 h.
720 The maximum release achieved at 48 h was 82.19 ± 4.75 % confirming high
721 bioavailability of CUR:HP β CD at the wound site to control bacterial infection
722 during the treatment period.



723 **Figure 10:** Release profile over 48 h from CUR:HP β CD-loaded-BC
724 hydrogels (n=6; error bars = SD).

725 After the release profile was evaluated, the disc diffusion assay was
726 undertaken to assess the antimicrobial activity of CUR:HP β CD-loaded-BC
727 hydrogels. The results revealed no anti-microbial activity against *S. aureus*
728 (Gram positive) for neat BC and HP β CD-loaded-BC which is in accordance
729 with literature [7,25,50,51]. However, CUR:HP β CD-loaded-BC hydrogels
730 demonstrated significant ($p<0.01$) antimicrobial activity (Fig. 11) (ZOI=
731 11.08 ± 0.90 mm) (n=12) compared to neat BC and HP β CD-loaded-BC. CUR
732 is well known for its antimicrobial properties against a broad range of
733 microorganisms [52-54]. Its antimicrobial activity ensues due to its ability to
734 interact with an essential prokaryotic cell division initiating protein (FtsZ)

735 [54,55]. Moreover, it has been identified to possess inhibitory effect against
736 sortase A, a membrane-associated transpeptidase that plays a crucial role in
737 modulating the ability of Gram-positive bacteria (including *S. aureus*) to
738 adhere to the host tissue and cause infection [53]. The disc diffusion results
739 confirmed that CUR maintained its antimicrobial feature even after
740 encapsulation in the HP β CD cavity demonstrating the potential use of
741 CUR:HP β CD as an antimicrobial for wound management.



742 **Figure 11:** Antimicrobial activity assessed by ZOI during the disc diffusion
743 assay for neat BC hydrogel, HP β CD-loaded-BC and CUR:HP β CD-loaded-
744 BC hydrogels against *S. aureus* (n=12; error bars = SD).

745 3.3.3. Anti-oxidant activity by DPPH assay

746 Oxidative stress has been identified, through preclinical and clinical studies, as
747 one of the major causes of nonhealing in chronic wounds [56]. CUR is
748 reported as a potent antioxidant due to its ability to reduce reactive oxygen
749 species such as super oxide radicals, lipid peroxyl radicals and hydroxyl
750 radicals [10,57]. Its antioxidant activity arises due to its ability to undergo H-
751 atom abstraction from its phenol groups giving rise to a stable, delocalised
752 radical species [56]. Several methods have been adopted to assess the free
753 radical scavenging potential of anti-oxidant substance and the DPPH assay is
754 still one of the routinely practiced method for this assessment. In the current
755 study, the antioxidant activity of CUR:HP β CD was assessed by this assay. The
756 reaction of DPPH radicals with antioxidant is a kinetic driven process which
757 varies for different antioxidants. In the current study, a fixed reaction time
758 mode of 30 min was adopted for estimation of the antioxidant activity [58].

759 The percent antioxidant effect for supramolecular CUR:HP β CD against DPPH
760 determined in the current study ranged from 12.06 \pm 0.014 - 79.75 \pm 0.001 % in
761 the range of 125-2000 μ g/mL and the IC₅₀ was found to be 1087.49 \pm 6.47
762 μ g/mL (n=3). It was found that HP β CD does not have antioxidant activity and
763 our results are in agreement with literature [59]. These finding confirmed that
764 the antioxidant activity of CUR stays preserved even after its encapsulation in
765 HP β CD cavity in the CUR:HP β CD inclusion complex. These findings are in
766 accordance with Aytac & Uyar (2017) [34]. These results advocate the
767 antioxidant potential of BC hydrogels loaded with CUR:HP β CD to reduce the
768 oxidative stress at the impaired wound site.

769 4. Conclusion:

770 The present study demonstrates the production, physicochemical characterisation, *in vitro*
771 biocompatibility and antimicrobial performance of biosynthetic CUR:HP β CD-loaded-BC
772 hydrogels for potential wound management applications. The physicochemical
773 characterisation confirmed the formation of IC of CUR:HP β CD with enhanced aqueous
774 solubility compared to free CUR. Varying the solvent volume ratios during the solvent
775 evaporation method, IC 75 emerged to be the best preparation method with the highest
776 encapsulation efficacy. The CUR:HP β CD-loaded-BC hydrogels demonstrated high light
777 transmission, a property that has a potential of clinical wound monitoring without the need
778 to remove the dressing. Moreover, these hydrogels offer optimum WVTR that could help
779 maintain the moist environment at the wound site. Their high moisture content,
780 biocompatibility (cytocompatibility and haemocompatibility), antimicrobial and
781 antioxidant properties advocates their potential application as hydrogel dressings for
782 chronic, infected wound management. These findings suggest that biosynthetic
783 CUR:HP β CD-loaded-BC hydrogels could represent an alternative in the dressing
784 landscape for wound management.

785 Acknowledgement:

786 The authors would like to thank Brian Johnston, Kate Butcher and Surila Darbar for their
787 kind assistance. This research was partially supported by the European Regional
788 Development Fund Project EnTRESS No 01R16P00718. Abhishek Gupta would like to
789 thank the University of Wolverhampton for financial support for his PhD research.

790 Conflict of interest

791 The authors confirm no conflict of interest. The authors alone are responsible for the
792 content and writing of the article.

793 **Appendix A. Supporting material**

794 Supplementary material related to this article can be found in this section.

795

796 **5. References**

797

- 798 1. A. Gupta, M. Kowalczyk, W. Heaselgrave, S.T. Britland, C. Martin, I. Radecka, The
799 production and application of hydrogels for wound management: A review, *Eur. Polym.*
800 *J.* 111 (2019) 134–151. doi:10.1016/j.eurpolymj.2018.12.019.
- 801 2. C. Martin, W. Low, A. Gupta, M. Amin, I. Radecka, S. Britland, P. Raj, K. Kenward,
802 Strategies for Antimicrobial Drug Delivery to Biofilm, *Curr. Pharm. Des.* 21 (2014) 43–
803 66. doi:10.2174/1381612820666140905123529.
- 804 3. K. Vowden, P. Vowden, Wound dressings: principles and practice, *Surg.* 35 (2017) 489–
805 494. doi:10.1016/j.mpsur.2017.06.005.
- 806 4. T. Abdelrahman, H. Newton, Wound dressings: principles and practice, *Surg.* 29 (2011)
807 491–495. doi:10.1016/j.mpsur.2011.06.007.
- 808 5. G.D. Winter, Formation of the Scab and the Rate of Epithelization of Superficial Wounds
809 in the Skin of the Young Domestic Pig, *Nature.* 193 (1962) 293–294.
810 doi:10.1038/193293a0.
- 811 6. J. Koehler, F.P. Brandl, A.M. Goepferich, Hydrogel wound dressings for bioactive
812 treatment of acute and chronic wounds, *Eur. Polym. J.* 100 (2018) 1–11.
813 doi:10.1016/j.eurpolymj.2017.12.046.
- 814 7. A. Gupta, W.L. Low, I. Radecka, S.T. Britland, M. Mohd Amin Cairul Iqbal, C. Martin,
815 Characterisation and in vitro antimicrobial activity of biosynthetic silver-loaded bacterial
816 cellulose hydrogels, *J. Microencapsul.* 33 (2016) 725–734.
817 doi:10.1080/02652048.2016.1253796.
- 818 8. H. Hamedi, S. Moradi, S.M. Hudson, A.E. Tonelli, Chitosan based hydrogels and their
819 applications for drug delivery in wound dressings: A review, *Carbohydr. Polym.* 199
820 (2018) 445–460. doi:10.1016/j.carbpol.2018.06.114.
- 821 9. D. Zmejkoski, D. Spasojević, I. Orlovska, N. Kozyrovska, M. Soković, J. Glamočlija, S.
822 Dmitrović, B. Matović, N. Tasić, V. Maksimović, M. Sosnin, K. Radotić, Bacterial
823 cellulose-lignin composite hydrogel as a promising agent in chronic wound healing, *Int. J.*
824 *Biol. Macromol.* 118 (2018) 494–503. doi:10.1016/j.ijbiomac.2018.06.067.
- 825 10. D. Akbik, M. Ghadiri, W. Chrzanowski, R. Rohanzadeh, Curcumin as a wound healing
826 agent, *Life Sci.* 116 (2014) 1–7. doi:10.1016/j.lfs.2014.08.016.
- 827 11. A.E. Krausz, B.L. Adler, V. Cabral, M. Navati, J. Doerner, R.A. Charafeddine, D.
828 Chandra, H. Liang, L. Gunther, A. Clendaniel, S. Harper, J.M. Friedman, J.D.
829 Nosanchuk, A.J. Friedman, Curcumin-encapsulated nanoparticles as innovative
830 antimicrobial and wound healing agent, *Nanomedicine Nanotechnology, Biol. Med.* 11
831 (2015) 195–206. doi:10.1016/j.nano.2014.09.004.
- 832 12. N. Wathoni, K. Motoyama, T. Higashi, M. Okajima, T. Kaneko, H. Arima, Enhancement
833 of curcumin wound healing ability by complexation with 2-hydroxypropyl- γ -cyclodextrin
834 in sacran hydrogel film, *Int. J. Biol. Macromol.* 98 (2017) 268–276.
835 doi:10.1016/j.ijbiomac.2017.01.144.
- 836 13. E.I. Paramera, S.J. Konteles, V.T. Karathanos, Stability and release properties of
837 curcumin encapsulated in *Saccharomyces cerevisiae*, β -cyclodextrin and modified starch,
838 *Food Chem.* 125 (2011) 913–922. doi:10.1016/j.foodchem.2010.09.071.

- 839 14. E.M. Martin Del Valle, Cyclodextrins and their uses: a review, *Process Biochem.* 39
840 (2004) 1033–1046. doi:10.1016/s0032-9592(03)00258-9.
- 841 15. S.S. Jambhekar, P. Breen, Cyclodextrins in pharmaceutical formulations I: structure and
842 physicochemical properties, formation of complexes, and types of complex, *Drug Discov.*
843 *Today.* 21 (2016) 356–362. doi:10.1016/j.drudis.2015.11.017.
- 844 16. G. Dufour, B. Evrard, P. de Tullio, Rapid quantification of 2-hydroxypropyl- β -
845 cyclodextrin in liquid pharmaceutical formulations by ¹H nuclear magnetic resonance
846 spectroscopy, *Eur. J. Pharm. Sci.* 73 (2015) 20–28. doi:10.1016/j.ejps.2015.03.005.
- 847 17. S. V Kurkov, T. Loftsson, Cyclodextrins, *Int. J. Pharm.* 453 (2013) 167–180.
848 doi:10.1016/j.ijpharm.2012.06.055.
- 849 18. M.M. Yallapu, M. Jaggi, S.C. Chauhan, β -Cyclodextrin-curcumin self-assembly enhances
850 curcumin delivery in prostate cancer cells, *Colloids Surfaces B Biointerfaces.* 79 (2010)
851 113–125. doi:10.1016/j.colsurfb.2010.03.039.
- 852 19. P.R.K. Mohan, G. Sreelakshmi, C. V Muraleedharan, R. Joseph, Water soluble
853 complexes of curcumin with cyclodextrins: Characterization by FT-Raman spectroscopy,
854 *Vib. Spectrosc.* 62 (2012) 77–84. doi:10.1016/j.vibspec.2012.05.002.
- 855 20. S. Hestrin, M. Schramm, Synthesis of cellulose by *Acetobacter xylinum*. 2. Preparation of
856 freeze-dried cells capable of polymerizing glucose to cellulose, *Biochem. J.* 58 (1954)
857 345–352. doi:10.1042/bj0580345.
- 858 21. C. Jantararat, P. Sirathanarun, S. Ratanapongsai, P. Watcharakan, S. Sunyapong, A. Wadu,
859 Curcumin-Hydroxypropyl- β -Cyclodextrin Inclusion Complex Preparation
860 Methods: Effect of Common Solvent Evaporation, Freeze Drying, and pH Shift on
861 Solubility and Stability of Curcumin, *Trop. J. Pharm. Res.* 13 (2014) 1215.
862 doi:10.4314/tjpr.v13i8.4.
- 863 22. H.E. Gottlieb, V. Kotlyar, A. Nudelman, NMR Chemical Shifts of Common Laboratory
864 Solvents as Trace Impurities, *J. Org. Chem.* 62 (1997) 7512–7515.
865 doi:10.1021/jo971176v.
- 866 23. ASTM E96 / E96M-16. Standard Test Methods for Water Vapor Transmission of
867 Materials, 2016.
- 868 24. S. Hu, X. Cai, X. Qu, B. Yu, C. Yan, J. Yang, F. Li, Y. Zheng, X. Shi, Preparation of
869 biocompatible wound dressings with long-term antimicrobial activity through covalent
870 bonding of antibiotic agents to natural polymers, *Int. J. Biol. Macromol.* 123 (2019)
871 1320–1330. doi:10.1016/j.ijbiomac.2018.09.122.
- 872 25. A. Gupta, W.L. Low, S.T. Britland, I. Radecka, C. Martin, Physicochemical
873 characterisation of biosynthetic bacterial cellulose as a potential wound dressing material,
874 *British J. Phar.* 2 (2017) S37-38. doi: 10.5920/bjpharm.2017.27.
- 875 26. L.-O. Lamke, G.E. Nilsson, H.L. Reithner, The evaporative water loss from burns and the
876 water-vapour permeability of grafts and artificial membranes used in the treatment of
877 burns, *Burns.* 3 (1977) 159–165. doi:10.1016/0305-4179(77)90004-3.
- 878 27. B. Balakrishnan, M. Mohanty, P. umashankar, A. Jayakrishnan, Evaluation of an in situ
879 forming hydrogel wound dressing based on oxidized alginate and gelatin, *Biomaterials.*
880 26 (2005) 6335–6342. doi:10.1016/j.biomaterials.2005.04.012.
- 881 28. T. Takao, F. Kitatani, N. Watanabe, A. Yagi, K. Sakata, A Simple Screening Method for
882 Antioxidants and Isolation of Several Antioxidants Produced by Marine Bacteria from
883 Fish and Shellfish, *Biosci. Biotechnol. Biochem.* 58 (1994) 1780–1783.
884 doi:10.1271/bbb.58.1780.

- 885 29. Z. Chen, R. Bertin, G. Frolidi, EC50 estimation of antioxidant activity in DPPH assay
886 using several statistical programs, *Food Chem.* 138 (2013) 414–420.
887 doi:10.1016/j.foodchem.2012.11.001.
- 888 30. L. Zhao, L. Kang, Y. Chen, G. Li, L. Wang, C. Hu, P. Yang, Spectral study on
889 conformation switchable cationic calix[4]carbazole serving as curcumin container,
890 stabilizer and sustained-delivery carrier, *Spectrochim. Acta Part A Mol. Biomol.*
891 *Spectrosc.* 193 (2018) 276–282. doi:10.1016/j.saa.2017.12.037.
- 892 31. Y. Sun, L. Du, Y. Liu, X. Li, M. Li, Y. Jin, X. Qian, Transdermal delivery of the in situ
893 hydrogels of curcumin and its inclusion complexes of hydroxypropyl- β -cyclodextrin for
894 melanoma treatment, *Int. J. Pharm.* 469 (2014) 31–39.
895 doi:10.1016/j.ijpharm.2014.04.039.
- 896 32. N. Li, N. Wang, T. Wu, C. Qiu, X. Wang, S. Jiang, Z. Zhang, T. Liu, C. Wei, T. Wang,
897 Preparation of curcumin-hydroxypropyl- β -cyclodextrin inclusion complex by
898 cosolvency-lyophilization procedure to enhance oral bioavailability of the drug, *Drug*
899 *Dev. Ind. Pharm.* 44 (2018) 1966–1974. doi:10.1080/03639045.2018.1505904.
- 900 33. A. Radjaram, A.F. Hafid, D. Setyawan, Dissolution enhancement of curcumin by
901 hydroxypropyl- β -cyclodextrin complexation. *Int. J. Phar. and Pharma. Sci.* 5, (2013) 401-
902 405.
- 903 34. Z. Aytac, T. Uyar, Core-shell nanofibers of curcumin/cyclodextrin inclusion complex and
904 polylactic acid: Enhanced water solubility and slow release of curcumin, *Int. J. Pharm.*
905 518 (2017) 177–184. doi:10.1016/j.ijpharm.2016.12.061.
- 906 35. C.-M. Hsu, S.-C. Yu, F.-J. Tsai, Y. Tsai, Enhancement of rhubarb extract solubility and
907 bioactivity by 2-hydroxypropyl- β -cyclodextrin, *Carbohydr. Polym.* 98 (2013) 1422–1429.
908 doi:10.1016/j.carbpol.2013.07.029.
- 909
- 910 36. P. Mura, Analytical techniques for characterization of cyclodextrin complexes in the solid
911 state: A review, *J. Pharm. Biomed. Anal.* 113 (2015) 226–238.
912 doi:10.1016/j.jpba.2015.01.058.
- 913 37. Z. Di, Z. Shi, M.W. Ullah, S. Li, G. Yang, A transparent wound dressing based on
914 bacterial cellulose whisker and poly(2-hydroxyethyl methacrylate), *Int. J. Biol.*
915 *Macromol.* 105 (2017) 638–644. doi:10.1016/j.ijbiomac.2017.07.075.
- 916 38. S. Tyeb, N. Kumar, A. Kumar, V. Verma, Flexible agar-sericin hydrogel film dressing for
917 chronic wounds, *Carbohydr. Polym.* 200 (2018) 572–582.
918 doi:10.1016/j.carbpol.2018.08.030.
- 919 39. H. Zhang, X. Luo, H. Tang, M. Zheng, F. Huang, A novel candidate for wound dressing:
920 Transparent porous maghemite/cellulose nanocomposite membranes with controlled
921 release of doxorubicin from a simple approach, *Mater. Sci. Eng. C.* 79 (2017) 84–92.
922 doi:10.1016/j.msec.2017.05.019.
- 923 40. H. Shahbazi, M. Tataei, M.H. Enayati, A. Shafeiey, M.A. Malekabadi, Structure-
924 transmittance relationship in transparent ceramics, *J. Alloys Compd.* 785 (2019) 260–285.
925 doi:10.1016/j.jallcom.2019.01.124.
- 926 41. Z. Tehrani, H.R. Nordli, B. Pukstad, D.T. Gethin, G. Chinga-Carrasco, Translucent and
927 ductile nanocellulose-PEG bionanocomposites—A novel substrate with potential to be

- 928 functionalized by printing for wound dressing applications, *Ind. Crops Prod.* 93 (2016)
929 193–202. doi:10.1016/j.indcrop.2016.02.024.
- 930
- 931 42. H. Adeli, M.T. Khorasani, M. Parvazinia, Wound dressing based on electrospun
932 PVA/chitosan/starch nanofibrous mats: Fabrication, antibacterial and cytocompatibility
933 evaluation and in vitro healing assay, *Int. J. Biol. Macromol.* 122 (2019) 238–254.
934 doi:10.1016/j.ijbiomac.2018.10.115.
- 935 43. ASTM F756-17. Standard Practice for Assessment of Hemolytic Properties of Materials.
936 2017
- 937 44. E.A. Kamoun, E.-R.S. Kenawy, T.M. Tamer, M. El-Meligy, M.S. Mohy Eldin, Poly
938 (vinyl alcohol)-alginate physically crosslinked hydrogel membranes for wound dressing
939 applications: Characterization and bio-evaluation, *Arab. J. Chem.* 8 (2015) 38–47.
940 doi:10.1016/j.arabjc.2013.12.003.
- 941 45. M.E. Hiro, Y.N. Pierpont, F. Ko, T.E. Wright, M.C. Robson, W.G. Payne, Comparative
942 evaluation of silver-containing antimicrobial dressings on in vitro and in vivo processes
943 of wound healing. *Eplasty* 12 (2012) 409-419.
- 944 46. S.-B. Zou, W.-Y. Yoon, S.-K. Han, S.-H. Jeong, Z.-J. Cui, W.-K. Kim, Cytotoxicity of
945 silver dressings on diabetic fibroblasts, *Int. Wound J.* 10 (2012) 306–312.
946 doi:10.1111/j.1742-481x.2012.00977.x.
- 947 47. M. Amirthalingam, N. Kasinathan, S. Mutalik, N. Udupa, In vitro biocompatibility and
948 release of curcumin from curcumin microcomplex-loaded chitosan scaffold, *J.*
949 *Microencapsul.* 32 (2015) 364–371. doi:10.3109/02652048.2015.1028496.
- 950 48. A. Kurniawan, F. Gunawan, A.T. Nugraha, S. Ismadji, M.-J. Wang, Biocompatibility and
951 drug release behavior of curcumin conjugated gold nanoparticles from aminosilane-
952 functionalized electrospun poly(N -vinyl-2-pyrrolidone) fibers, *Int. J. Pharm.* 516 (2017)
953 158–169. doi:10.1016/j.ijpharm.2016.10.067.
- 954 49. X. Liu, L. You, S. Tarafder, L. Zou, Z. Fang, J. Chen, C.H. Lee, Q. Zhang, Curcumin-
955 releasing chitosan/aloe membrane for skin regeneration, *Chem. Eng. J.* 359 (2019) 1111–
956 1119. doi:10.1016/j.cej.2018.11.073
- 957
- 958 50. G. Yang, J. Xie, F. Hong, Z. Cao, X. Yang, Antimicrobial activity of silver nanoparticle
959 impregnated bacterial cellulose membrane: Effect of fermentation carbon sources of
960 bacterial cellulose, *Carbohydr. Polym.* 87 (2012) 839–845.
961 doi:10.1016/j.carbpol.2011.08.079.
- 962 51. O. Aleem, B. Kuchekar, Y. Pore, S. Late, Effect of β -cyclodextrin and hydroxypropyl β -
963 cyclodextrin complexation on physicochemical properties and antimicrobial activity of
964 cefdinir, *J. Pharm. Biomed. Anal.* 47 (2008) 535–540. doi:10.1016/j.jpba.2008.02.006.
- 965 52. S.-H. Mun, D.-K. Joung, Y.-S. Kim, O.-H. Kang, S.-B. Kim, Y.-S. Seo, Y.-C. Kim, D.-S.
966 Lee, D.-W. Shin, K.-T. Kweon, D.-Y. Kwon, Synergistic antibacterial effect of curcumin
967 against methicillin-resistant *Staphylococcus aureus*, *Phytomedicine.* 20 (2013) 714–718.
968 doi:10.1016/j.phymed.2013.02.006.

- 969 53. P. Hu, P. Huang, M.W. Chen, Curcumin reduces *Streptococcus mutans* biofilm formation
970 by inhibiting sortase A activity, *Arch. Oral Biol.* 58 (2013) 1343–1348.
971 doi:10.1016/j.archoralbio.2013.05.004.
- 972 54. A.C. da Silva, P.D. de F. Santos, J.T. do P. Silva, F.V. Leimann, L. Bracht, O.H.
973 Gonçalves, Impact of curcumin nanoformulation on its antimicrobial activity, *Trends*
974 *Food Sci. Technol.* 72 (2018) 74–82. doi:10.1016/j.tifs.2017.12.004.
- 975 55. D. Rai, J.K. Singh, N. Roy, D. Panda, Curcumin inhibits FtsZ assembly: an attractive
976 mechanism for its antibacterial activity, *Biochem. J.* 410 (2008) 147–155.
977 doi:10.1042/bj20070891.
- 978 56. C. Mohanty, S.K. Sahoo, Curcumin and its topical formulations for wound healing
979 applications, *Drug Discov. Today.* 22 (2017) 1582–1592.
980 doi:10.1016/j.drudis.2017.07.001
- 981 57. S. Jena, C. Anand, G.B.N. Chainy, J. Dandapat, Induction of oxidative stress and
982 inhibition of superoxide dismutase expression in rat cerebral cortex and cerebellum by
983 PTU-induced hypothyroidism and its reversal by curcumin, *Neurol. Sci.* 33 (2011) 869–
984 873. doi:10.1007/s10072-011-0853-4.
- 985
- 986 58. K. Mishra, H. Ojha, N.K. Chaudhury, Estimation of antiradical properties of antioxidants
987 using DPPH assay: A critical review and results, *Food Chem.* 130 (2012) 1036–1043.
988 doi:10.1016/j.foodchem.2011.07.127.
- 989 59. J. Rakmai, B. Cheirsilp, J.C. Mejuto, J. Simal-Gándara, A. Torrado-Agrasar, Antioxidant
990 and antimicrobial properties of encapsulated guava leaf oil in hydroxypropyl-beta-
991 cyclodextrin, *Ind. Crops Prod.* 111 (2018) 219–225. doi:10.1016/j.indcrop.2017.10.027.